



Rika Taslim <rikataslim@gmail.com>

---

## [ANSN-2022-0119] - Manuscript Submitted

1 message

---

**NVT Secretariat of ANSN** <onbehalf@manuscriptcentral.com>

Fri, Jun 17, 2022 at 11:16 AM

Reply-To: journal@ans.vast.vn

To: rikataslim@gmail.com

17-Jun-2022

Dear Dr. Taslim:

Your manuscript entitled "Agricultural Bio-waste-derived Hierarchical Porous Carbon Nanofiber for High-performance Supercapacitors" has been successfully submitted online and is presently being given full consideration for publication in the Advances in Natural Sciences: Nanoscience and Nanotechnology (ANSN).

Your manuscript ID is ANSN-2022-0119.

Please mention the above manuscript ID in all future correspondence or when calling the office for questions. If there are any changes in your street address or e-mail address, please log in to ScholarOne Manuscripts at <https://mc04.manuscriptcentral.com/vastansn> and edit your user information as appropriate.

You can also view the status of your manuscript at any time by checking your Author Center after logging in to <https://mc04.manuscriptcentral.com/vastansn>.

Thank you for submitting your manuscript to the Advances in Natural Sciences: Nanoscience and Nanotechnology. If you have any questions, feel free to contact us at [journal@ans.vast.vn](mailto:journal@ans.vast.vn).

Sincerely,

Editorial Office

Advances in Natural Sciences: Nanoscience and Nanotechnology (ANSN)

Jointly published by VAST (VN) and IOP (UK)

Abstracted in Web of Science (ESCI), Scopus, Chemical Abstracts,...

E-mail: [journal@ans.vast.vn](mailto:journal@ans.vast.vn)

Homepage: <https://iopscience.iop.org/ansn>; <https://ans.vast.vn/>

Manuscript submission: <https://mc04.manuscriptcentral.com/vastansn>



# ADVANCES IN NATURAL SCIENCES: NANOSCIENCE AND NANOTECHNOLOGY

## Agricultural Bio-waste-derived Hierarchical Porous Carbon Nanofiber for High-performance Supercapacitors

Journal:	<i>Advances in Natural Sciences: Nanoscience and Nanotechnology</i>
Manuscript ID	Draft
Manuscript Type:	Original Article
Date Submitted by the Author:	n/a
Complete List of Authors:	Taslim, Rika; State Islamic University Sultan Syarif Kasim, Department of Industrial Engineering Taer, Erman; University of Riau - Bina Widya Campus, Department of physics Halbi, Suryandri; State Islamic University Sultan Syarif Kasim, Department of Industrial Engineering Apriwandi, Apriwandi; University of Riau - Binawidja Campus, Department of Physics
Keywords:	Nanofiber, Porous carbon, electrode material, Supercapacitor
Classification numbers:	5.16, 5.18

SCHOLARONE™  
Manuscripts

## Agricultural Bio-waste-derived Hierarchical Porous Carbon Nanofiber for High-performance Supercapacitors

Rika Taslim<sup>1,\*</sup>, Erman Taer<sup>2</sup>, Suryandri Halbi<sup>1</sup>, Apriwandi Apriwandi<sup>2</sup>

<sup>1</sup> Department of Industrial Engineering, State Islamic University of Sultan Syarif Kasim, 28293 Simpang Baru, Riau, Indonesia

<sup>2</sup> Department of Physics, Faculty of Mathematics and Natural Sciences, University of Riau, 28293 Simpang Baru, Riau, Indonesia

Email: [rikataslim@gmail.com](mailto:rikataslim@gmail.com)

**Abstract.** Activated carbon-derived biomass materials widely used as energy storage supercapacitors have a hierarchical pore 3D structure, large specific surface area, controllable surface morphology, as well as an in-expensive and non-complex approach. Therefore, this study aims to develop a novel, simple, efficient, and low-cost method to prepare hierarchical porous carbon nanofiber derived from corn silks (CSAC) through a one-step carbonization-physical activation process. The carbon precursors were activated by KOH solution at a high pyrolysis temperature to prepare activated porous nanofibers as an electrode material for supercapacitors without using binders. This study focused on the effect of different activation temperatures of 600, 700, 800, and 900°C on the production of highly porous carbon nanofiber. An enhancement mechanism is proposed, which not only performed high nanofiber structures to possess the large specific active surface area to enhance energy density but also achieve micro-mesopores combination to realize fast ion-transport channels for boosting high power density. A maximum specific surface area of approximately 1096.951 m<sup>2</sup> g<sup>-1</sup> was achieved by CSAC7. Furthermore, the electrochemical performance was evaluated using 1 M H<sub>2</sub>SO<sub>4</sub> solution as an electrolyte through a novel two-electrode binder-free system. The electrode materials produced a maximum specific capacitance of 237 F g<sup>-1</sup> at a current density of 1 A g<sup>-1</sup>. These excellent characteristics show that the synthetic approach has a great potential for fabricating high-performance supercapacitors.

Keywords: Nanofiber, porous carbon, electrode material, supercapacitor.

Classification numbers: 5.16, 5.18

## 1. Introduction

Supercapacitors are globally considered as superior storage devices due to the higher energy and power density compared to batteries, capacitors, and fuel cells [1]. In addition, they function as suitable materials for electrical components, pulse laser systems, and other electronic devices [2]. Supercapacitors are also directly utilized or combined with batteries for certain electrical facilities, such as electric braking, starters, vehicle, and generators [3]. The electric double-layer capacitors (EDLC) are considered to be the best type due to the variable and adaptable active materials, low cost, abundant availability, superior material properties, maximum electrolyte flow rate, high operating temperature and conductivity, compatible with a variety of low and high current components, environmentally friendly, and relatively safer [4]. However, supercapacitors still have various challenges such as the relatively low energy compared to the high power density, expensive active materials, and complex synthetic methods. In different studies, the energy density of supercapacitors has been increased with various approaches, but with a reduced power density. The main key to improving the performance of supercapacitors is the active electrode material, followed by the electrolyte and separator [5]. Three groups of active electrode materials have been reported including conduction polymers, metal oxides, and carbon [6]. Conducting polymer materials and metal oxides were used to successfully increase the energy density up to 200 Wh kg<sup>-1</sup> [7]. This is several times greater than the result from other studies in the last decade. However, both materials require complex, complicated, corrosive, and toxic instruments, hence, they are not recommended for environmentally friendly mass production. Therefore, activated carbon from biomass and bio-organic waste is more promising as it has superior and attractive characteristics including abundant availability, renewability, easy fabrication, and low cost [8,9]. Activated carbon materials also have a good performance in increasing and maintaining energy density, although the energy density produced is still relatively low

1  
2  
3 compared to metal oxides and conduction polymers. [10,11] Additionally, biomass precursors  
4 rich in structurally diverse porosity and significant heteroatoms provide a large number of  
5 active ion contacts and facilitate the transport of electrolytic ion charges in various pores  
6 including micro-, meso-, and macro- leading to a high performance of energy and balanced  
7 power density [12]. Moreover, the 3D hierarchical pore structure obtained from the biomass-  
8 derived activated carbon has been shown to increase the energy density up to 5 times coupled  
9 with a high power density [13]. Hierarchical porous carbon consisting of micro-, meso-, and  
10 macropores are obtained from various biomass precursors such as orange peel [14], pineapple  
11 leaves [15], rice husk [16], ginger waste [17], peanut shells [18], bamboo stem [19], and  
12 jujube fruit [20]. The peanut shell agricultural biomass produced activated carbon having a  
13 3D hierarchical pore structure as well as abundant micropores and mesopores with surface  
14 area=2014.6 m<sup>2</sup> g<sup>-1</sup>. Activated carbon is prepared by a new and low-cost method using  
15 ZnCl<sub>2</sub>/CO<sub>2</sub> activation which produced a specific capacitance of 310 F g<sup>-1</sup> in a 3-electrode  
16 system [21]. Shang *et al.*, (2021) obtained activated carbon from chitin (*Portunus*  
17 *trituberculatus* Crab) waste [22], which was converted into hierarchical porous carbon  
18 through ZIF-8 nanoparticles bio-template followed by high-temperature carbonization,  
19 leading to a specific capacitance of 182 F g<sup>-1</sup>. Similar results were also obtained from  
20 different biomass precursors such as cauliflower which produced a unique hierarchical pore  
21 structure using KOH activation at 700°C high-temperature simple which possessed a high  
22 surface area of 2061 m<sup>2</sup> g<sup>-1</sup> [23]. However, the activated carbons obtained from the above  
23 precursors are prepared in powder form, hence, they require synthetic binders and insulators  
24 to test the electrochemical properties. Although the counter electrodes used are good  
25 conduction materials, it is still considered to reduce the efficiency. Also, the template/bio-  
26 template method often used to ascertain the 3D pore structure is a relatively risky technique  
27 because the final step requires more treatment to remove the by-products. On the other hand,  
28  
29  
30  
31  
32  
33  
34  
35  
36  
37  
38  
39  
40  
41  
42  
43  
44  
45  
46  
47  
48  
49  
50  
51  
52  
53  
54  
55  
56  
57  
58  
59  
60

1  
2  
3 corn silk agricultural biomass has high potential as a hierarchical porous carbon precursor.  
4  
5 The basic fibrous structure allows the discovery of dense nanofibers on activated carbon,  
6  
7 thereby adding to its renewability. Although the use of corn silk as a starting material for  
8  
9 activated carbon in supercapacitors has been previously reported, the method of preparation  
10  
11 using binders through a relatively complicated technique is considered to limit its novelty.  
12  
13 Therefore, this study aims to prepare binder-free activated carbon through a novel one-step  
14  
15 activation of KOH/CO<sub>2</sub>. The chosen strategy has been shown to produce higher capacitance  
16  
17 compared to Mitravinda *et al.* (2018) [24] which used different methods and possesses higher  
18  
19 energy density compared to a study by Zhou *et al.* (2020) [25]. In addition, we selected  
20  
21 H<sub>2</sub>SO<sub>4</sub> aqueous electrolytes because of their advantages including the highest ionic  
22  
23 concentration, highest conductivity, and low viscosity compared to other aqueous  
24  
25 electrolytes. In result, the optimum specific capacitance of activated carbon obtained is 237 F  
26  
27 g<sup>-1</sup> with a maximum energy density of 18.19 Wh kg<sup>-1</sup> in an aqueous electrolyte of 1 M  
28  
29 H<sub>2</sub>SO<sub>4</sub>.  
30  
31  
32  
33

## 34 35 **2. Materials and methods**

### 36 37 **2.1. Materials**

38  
39 The corn silks (CS) were initially obtained from the traditional plantations of the  
40  
41 Kampar community, Riau and then cut into small pieces within a range of 2 cm, cleaned, and  
42  
43 sundried for 48 hours to obtain dry samples. Furthermore, the samples were pre-carbonized  
44  
45 and crushed using a crusher machine to obtain dried corn silk powder. The KOH activating  
46  
47 agent, HCl, and aqueous electrolyte H<sub>2</sub>SO<sub>4</sub> were obtained from Merck KGaA, 4271  
48  
49 Darmstadt, Germany, and Panreac Quimica Sau, Espana, while deionized water (DI) as a  
50  
51 material for neutralizing samples was made on a lab scale. The organic separator from the  
52  
53 duck eggshell membrane was extracted with 1 M HCl solution.  
54  
55  
56  
57

### 58 59 **2.2. Synthesis of carbon pellets**

1  
2  
3 30 g of dried corn silks powder was dissolved with a 0.5 m/L KOH solution on a  
4 hotplate at 300 rpm for 2 hours. The sample was precipitated and dried in an oven at 110 °C,  
5  
6 while the corn silk powder was converted into pellets using a hydraulic press without using  
7  
8 any adhesive material, hence, the adhesive properties of the pure powder were derived  
9  
10 originally from the sample. A total of 20 pellets samples were prepared for pyrolysis using  
11  
12 carbonization in the N<sub>2</sub> gas environment and physical activation with CO<sub>2</sub> in the furnace tube.  
13  
14 In addition, the pyrolysis process began from a temperature of 30° C to 600 °C in N<sub>2</sub> gas and  
15  
16 then increased to 900 °C in a CO<sub>2</sub> environment. Four different carbonization temperatures  
17  
18 were applied namely 600 °C, 700 °C, 800 °C, and 900 °C. Moreover, to facilitate data  
19  
20 interpretation, samples were labeled CSAC-x, CSAC was corn silk activated carbon (CSAC),  
21  
22 while x was the number 6, 7, 8, and 9 indicating carbonization at the four temperatures. The  
23  
24 pelleted carbon samples were neutralized using DI water.  
25  
26  
27  
28  
29

### 30 **2.3. Characterization of materials**

31  
32  
33 The carbon pellets' density was evaluated based on changes in mass, thickness, and  
34  
35 diameter during the pyrolysis process through standard equations. Furthermore, the  
36  
37 amorphous properties of the samples were characterized using the XRD (X-ray diffraction)  
38  
39 technique at an angle range of 5-60 ° in a Cu K $\alpha$  radiation source (Phillips expert powder  
40  
41 instrument). Surface morphology and variation of sample elements were also examined  
42  
43 through the SEM-EDS (Scanning electron microscopy-energy dispersive spectroscopy)  
44  
45 technique using the JEOL-JSM-LA-3600 instrument at a voltage of 15Kv. Additionally, the  
46  
47 specific surface area and pore diversity were determined through the N<sub>2</sub> gas absorption  
48  
49 technique and evaluated using BET and BJH calculations.  
50  
51  
52

### 53 **2.4. Supercapacitor electrochemical performance**

54  
55  
56 The electrochemical properties of the supercapacitor were evaluated in two-electrode  
57  
58 configurations. The supercapacitor cells were made in the form of sandwich layers consisting  
59  
60

of a cell body made of acrylic, stainless steel current collector, pelleted carbon electrodes, and an organic separator from the duck eggshell membrane. The cyclic voltammetry (CV) and galvanostatic charge-discharge (GCD) methods are techniques commonly used in evaluating specific capacitance, as well as energy and power density. CV was evaluated using the CV-UR Rad-Er 1380 instrument at a constant voltage range of 0-1.0V at a scan rate of 1 mV s<sup>-1</sup>, while GCD used the 2018 CD-UR Rad-Er at a fixed current of 1 A, both instruments were calibrated with a mean error of ± 6.01%.

### 3. Results and discussions

Crystal phase change properties of corn silk-based hierarchical porous carbon were reviewed using the powder X-ray diffraction (XRD) method. The XRD pattern with different physical activation temperatures particularly between 700 and 900 °C, are shown in Figure 1.

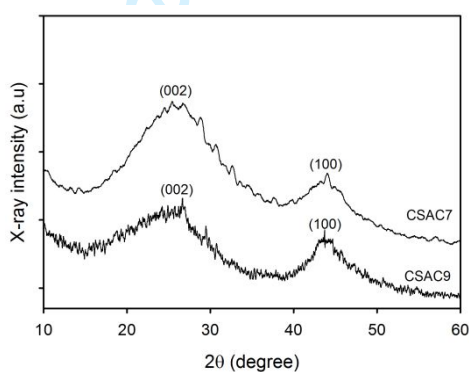


**Figure 1.** The XRD pattern of CSAC7 and CSAC9

The CSAC7 display two clearly confirmed broad peaks at  $2\theta$  angles  $24.34^\circ$  and  $43.92^\circ$  which correspond to the scattering planes 002 and 100. These characteristics show that the structure of the turbostratic/disturbed carbon has a high amorphous nature [26]. On the other hand, CSAC9 performed low broad peaks at angles of  $2\theta$   $24.86^\circ$  and  $44.13^\circ$  indicating the amorphous nature degraded towards graphitization due to high-temperature treatment. Furthermore, the most obvious broad peaks in the 002 reflection plane ranging between angle  $24.34^\circ$ - $24.86^\circ$  indicate a random aromatic sheet structure, while the 100 reflection plane from  $43.92^\circ$ - $44.13^\circ$  confirms the type of carbon that is close to the graphite structure, in this case,



1  
2  
3 the attenuation of the graphite structure towards the formation of a disturbed carbon structure  
4 [27,28]. The reflection planes 002 and 100 were attenuated from sample CSAC7 to CSAC9  
5  
6 as the high-temperature pyrolysis process from 700 to 900 °C tends to increase the random  
7  
8 disturbed structure of activated carbon, thereby initiating a better amorphous formation [29].  
9  
10 This property is important for improving the good hierarchical pore structures in carbon  
11  
12 samples. The morphological structure of activated carbon-based corn silk waste was  
13  
14 evaluated using the SEM method at a voltage of 15 kV. Figure 2 shows the morphological  
15  
16 structure with different physical activation temperatures of 600, 700, 800, and 900 °C. In  
17  
18 general, the outer surface structure of the sample is dominated by bulk materials, aggregation  
19  
20 and clumps of large wrinkled particles, while some parts display a different inner surface  
21  
22 structure for each temperature. At 600 °C (Figure 2a), the activated carbon consisted of  
23  
24 particle aggregations with surface wrinkles. Additionally, a larger zoom in Figure 3b shows  
25  
26 that the sample surface is relatively flat in each aggregation without any obvious pores.  
27  
28 Furthermore, physical activation at a higher temperature above 700 °C led to a better  
29  
30 decomposition into the basic components including hemicellulose, cellulose, lignin compared  
31  
32 to 600°C. This indicates a relatively different surface morphology as shown in Figure 2c-d.  
33  
34 Figure 3c shows the relatively dominant pore holes structure in the 64-7214 nm range. The  
35  
36 diverse pore structure including mesopores and macropores were confirmed at a larger  
37  
38 magnification area as shown in Figure 2d. Mesopores have a size ranging from 18-48 nm,  
39  
40 while macropores are in the range of 73-136 nm. However, micropore structures were not  
41  
42 found at this magnification. The combination of the mesoporous and macropore structures is  
43  
44 very advantageous in the smooth ion diffusion process as well as its absorption direction in  
45  
46 the form of 3D to increase and maintain the high energy and power density of the  
47  
48 supercapacitor respectively [10,30]. This analysis was further confirmed using cyclic  
49  
50 voltammetry.  
51  
52  
53  
54  
55  
56  
57  
58  
59  
60

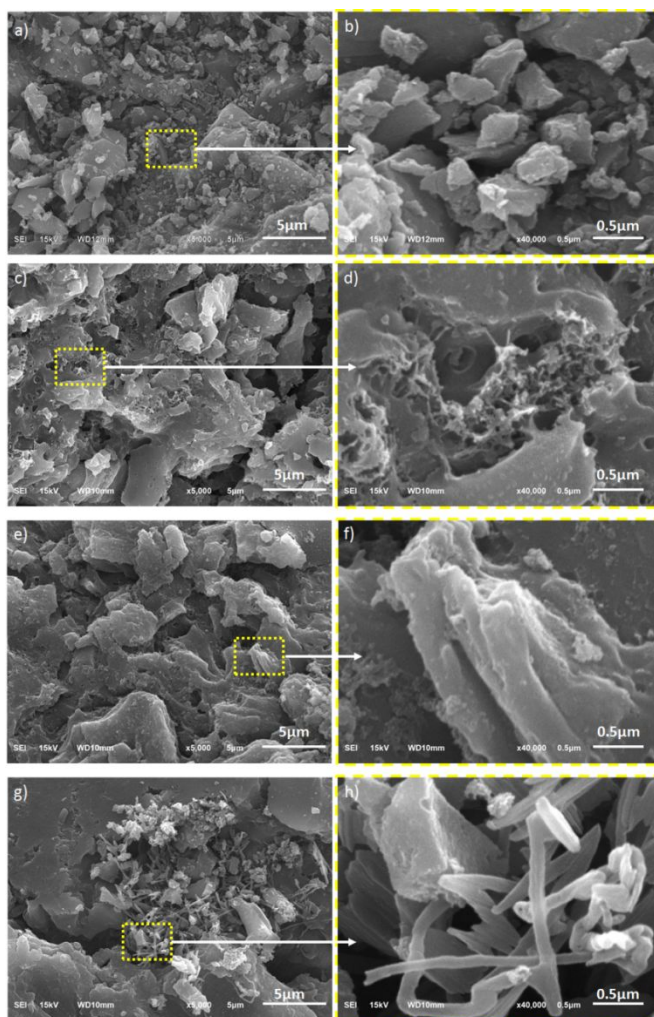


**Figure 2.** The SEM macrograph of CSAC6 in magnification of (a) 5000x, (b) 40000x, CSAC7 in magnification of (c) 5000x, (d) 40000x, CSAC8 in magnification of (e) 5000x, (f) 40000x, CSAC9 in magnification of (g) 5000x, (h) 40000x

An increase in the physical activation temperature of 800 °C in the CSAC8 sample shows a surface morphology filled with macropores which have a relatively large size less than 300 nm as shown in Figure 2e. In addition, Figure 2f shows a distinct morphology in which clustered tubular-rod-like structures are found. This is because the higher temperature porosity allows the breakdown of the main carbon structure derived from cellulose and lignin drastically. The rod shape is contributed from the basic structure of cellulose while the outer tubular shape is attributed to lignin [31]. This analysis has been reported in previous studies with different biomass precursors such as cassava petiole [32] and cacao shells [33].

Moreover, the temperature of 900°C maximized the basic decomposition process of cellulose and lignin to form a clear surface morphology of carbon fibers, as shown in Figure 2g-h. The diameter of the obtained nanofibers varied relatively in the range of 76 nm to 127 nm. The predominant nanofiber fiber allows well-connected pores in a relatively small size range [34]. These characteristics improve the high performance of supercapacitors. The elemental composition of porous activated carbon samples at activation temperatures of 700 °C and 900 °C for CSAC7 and CSAC9 was examined using energy dispersive spectroscopy (EDS) techniques in the energy range of 0-20 keV. Table 1 shows the elemental composition of the CSAC7 and CSAC9 samples in detail. Elemental carbon (C) has the highest percentage of approximately 83.7485-85.2755% followed by oxygen 8.0333-8.6075%, silicon (Si) 3.2471-3.1535%, potassium (K) 1.6359- 3.9428%, magnesium (Mg) 0.8317-0.7930%, and aluminum (Al) 0.4022-0.3290%.

**Table 2.** The elemental composition of CSAC7 and CSAC9

Element	CSCA7 (%)	CSAC9 (%)
Carbon (C)	85.2755	83.7485
Oxygen (O)	8.6075	8.0333
Silicon (Si)	3.2471	3.1535
Potassium (K)	1.6359	3.9428
Magnesium (Mg)	0.8317	0.7930
Aluminium (Al)	0.4022	0.3290

High-temperature pyrolysis of 700 C for CSAC7 showed the highest carbon composition of 85.2755%. This property is considered to increase the capacitive properties of the electrode material. Furthermore, the highest elemental oxygen was also found in the CSAC7 sample which contributed to the wettability of the material thereby initiating the pseudocapacitance effect [35]. An increase in the activation temperature up to 900C for CSAC9 reduced the percentage of carbon and oxygen in the sample. This is because the activation of high temperatures evaporates the constituent elements of the material in the

form of more H<sub>2</sub>O and CO<sub>2</sub>. Moreover, other elements such as Silicon, Potassium, Magnesium, and Aluminum are obtained in relatively low amounts from basic sources of biomass that have not been completely evaporated [36].

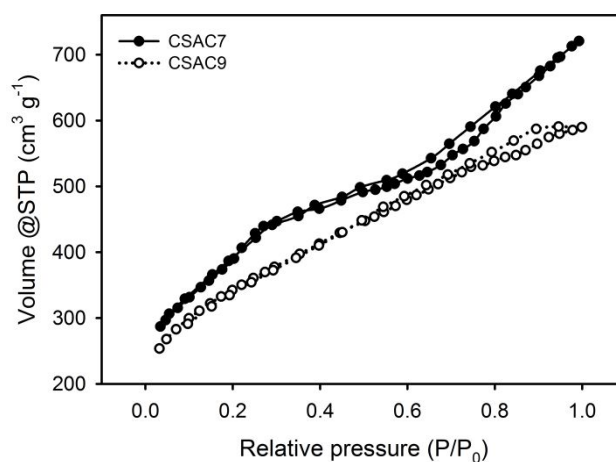


**Figure 3.** Nitrogen adsorption-desorption isotherms of CSAC7 and CSAC9

The analysis of nitrogen adsorption/desorption isotherms of corn silk-based hierarchical porous activated carbon at different pyrolysis temperatures are needed to evaluate the impact of pore structure and porosity properties. Figure 3 shows the N<sub>2</sub> adsorption-desorption isotherm curve of both samples, CSAC7 had significant N<sub>2</sub> adsorption at a relative pressure of  $0.0 < P/P_0 < 0.2$ , thereby confirming the relatively large number of micropores. Furthermore, the H4 type hysteresis loop was clearly shown over a relatively long relative pressure range of  $0.2 < P/P_0 < 0.9$  indicating uniform mesoporous characteristics at CSAC7 as presented in Table 2. The tail at high-pressure  $P/P_0 > 0.9$  shows the presence of macropores, but the addition of the physical activation temperature up to 900°C in CSAC9 showed a different N<sub>2</sub> isotherm absorption compared to CSAC7. Similar results were further confirmed through the N<sub>2</sub> gas absorption profile presented in Figure 3. The KOH reaction at a carbonization temperature of 700 °C showed the highest reduction in pellet density of 29.85% indicating that the CSAC7 sample has abundant pores for high performance of supercapacitor electrodes. The N<sub>2</sub> adsorption-desorption curve of CSAC9 shows a relatively linearly

increasing adsorption which is not too high at low pressure, thereby indicating the presence of low micropores. In addition, the H4 type hysteresis loop is not formed completely at a relatively short pressure range of  $P/P_0 = 0.6$  to 0.95 which is mainly due to the pores growing towards the larger one and is dominated by narrow bottle neck-like types with a larger inner surface [37] as shown in Table 2.

**Table 2.** Specific surface area, pore volume and average pores size of CSAC7 and CSAC9

Sample	$S_{\text{BET}}$ ( $\text{m}^2 \text{g}^{-1}$ )	$S_{\text{micro}}$ ( $\text{m}^2 \text{g}^{-1}$ )	$S_{\text{meso}}$ ( $\text{m}^2 \text{g}^{-1}$ )	$V_{\text{tot}}$ ( $\text{cm}^3 \text{g}^{-1}$ )	$V_{\text{micro}}$ ( $\text{cm}^3 \text{g}^{-1}$ )	$V_{\text{meso}}$ ( $\text{cm}^3 \text{g}^{-1}$ )	$D_{\text{aver}}$ (nm)
CSAC7	1096.951	531.087	565.864	1.115	0.314	0.801	4.06
CSAC9	744.818	423.360	321.458	0.9126	0.4476	0.465	3.15

The pore size distribution as presented in Figure 4 show that both samples have a combination of micropores and macropores. This result is relatively consistent with SEM which also confirms the hierarchical porous structure. CSAC7 has a structure of hierarchically connected 3D pores leading to the presence of mesopores with a peak at 3.89 nm. Furthermore, the chemical impregnation of KOH at 700°C high-temperature pyrolysis allows the precursor to produce a good combination of micropores and mesopores to improve the performance of the base electrode.

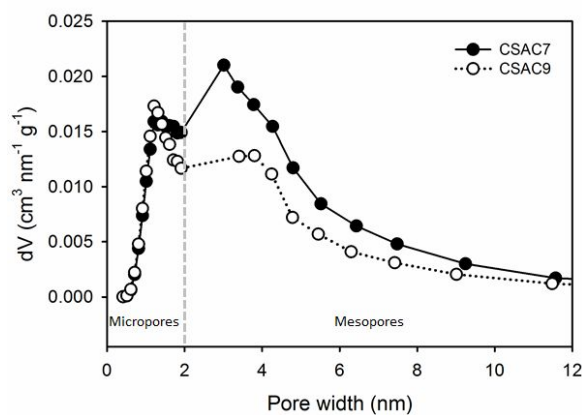
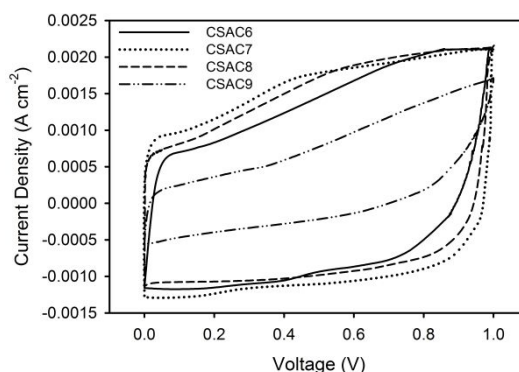


**Figure 4.** Pore sizes profile of CSAC7 and CSAC9

1  
2  
3 The microporous and mesoporous percentages of CSAC7 were 48.41% and 51.59% with  
4 a high surface area of  $1096.951 \text{ m}^2 \text{ g}^{-1}$ . The high surface area coupled with the combination  
5 of the hierarchically connected pores is believed to improve the electrochemical properties of  
6 supercapacitors [38]. In addition, the high mesoporous volume fraction potentially facilitates  
7 rapid ion transport and act as an electrolyte ion reservoir, thereby reducing the ion diffusion  
8 distance to the carbon surface, ensuring high rate capability and high power density.  
9 Moreover, CSAC9 displays a relatively similar pore size distribution with CSAC7 but is  
10 dominated by micropores with a percentage of 56.84%. KOH impregnation at higher  
11 temperatures up to  $900^\circ\text{C}$  allows degradation of carbon aggregation and erodes the main pore  
12 walls, thereby creating tubular and nanofiber structures. This simultaneously reduces the  
13 specific surface area of CSAC9 to  $744.818 \text{ m}^2 \text{ g}^{-1}$  with an average diameter of 3.15 nm as  
14 shown in Table 2. Nevertheless, the developed porosity properties of carbon materials are  
15 important for electrolyte ions' rapid transport and penetration [39]. These results are  
16 consistent with the SEM and density data.

17  
18  
19 The main parameters used to evaluate the electrochemical properties of hierarchical  
20 porous activated carbon include high specific capacitance, increased energy and fixed power  
21 density, as well as retention capacitance. Based on the  $\text{N}_2$  gas absorption analysis, the corn  
22 silk-based activated carbon has a combination of micropores and mesopores that is able to  
23 accommodate a relatively high charge of active ions and facilitate diffusion without  
24 obstruction at the electrode/electrolyte interface. The electrochemical performance of  
25 CSAC6, CSAC7, CSAC8, and CSAC9 based on different physical activation temperatures  
26 was evaluated with a two-electrode configuration in an aqueous electrolyte using cyclic  
27 voltammetry and galvanostatic charge-discharge techniques. Cyclic voltammetry (CV) curves  
28 at 600, 700, 800, and  $900^\circ\text{C}$  are shown in Figure 5. The CV profile exhibits a quasi-

1  
2  
3 rectangular shape, indicating the typical behavior of electrochemical double-layer type  
4  
5 supercapacitors (EDLC) in an aqueous electrolytic system at a scan rate of  $1 \text{ mV s}^{-1}$ .  
6  
7



8  
9  
10  
11  
12  
13  
14  
15  
16  
17  
18  
19  
20  
21 **Figure 5.** CV curve of CSAC6, CSAC7, CSAC8, and CSAC9

22  
23 In addition, the pseudocapacitance property was found to be relatively low as indicated by a  
24 spike in current density of the voltage ranging from 0.3-0.6V. This property is a contribution  
25 of the heteroatom and wettability properties of elemental oxygen in the sample. In general, all  
26 samples exhibited similar electrochemical properties. Using standard equations, the specific  
27 capacitances of CSAC6, CSAC7, CSAC8, and CSAC9 was evaluated to be 184, 211, 194,  
28 and 143  $\text{F g}^{-1}$ , respectively. An increase in the physical activation temperature improved the  
29 capacitive properties of the supercapacitor by  $211 \text{ F g}^{-1}$ . This is because the higher  
30 temperature of CSAC7 showed a relatively rich surface structure of mesopores and  
31 macropores, which provides a high surface area and diffusion path of ionic charge in all  
32 directions, thereby facilitating the high capacitive properties. This analysis is consistent with  
33 SEM results and  $\text{N}_2$  gas absorption in Figures 2 and 3. At  $800 \text{ }^\circ\text{C}$ , the surface structure of the  
34 capacitive properties was reduced to  $194 \text{ F g}^{-1}$ . This is because the increase in the physical  
35 activation temperature in the CSAC8 sample shows a surface morphology filled with  
36 macropores with a relatively large size less than  $300 \text{ nm}$ , as shown in Figure 2e. In addition,  
37 the morphology of the clustered tubular rod-like structure allows for fractures that narrow the  
38 ion transport pathways on the electrode surface. A further temperature is increased up to  $900$   
39  $^\circ\text{C}$  for CSAC9 allows the erosion and breakdown of the particle walls of carbon aggregation  
40  
41  
42  
43  
44  
45  
46  
47  
48  
49  
50  
51  
52  
53  
54  
55  
56  
57  
58  
59  
60

and rod-like structures to cover the existing pores, this reduced the capacitive properties to  $143 \text{ F g}^{-1}$ . Although the pore structure displays relatively dense nanofibers, as shown in Figure 2h, it is unable to maintain the 3D hierarchical pore distribution of micropores and mesopores thereby reducing the electrochemical properties.

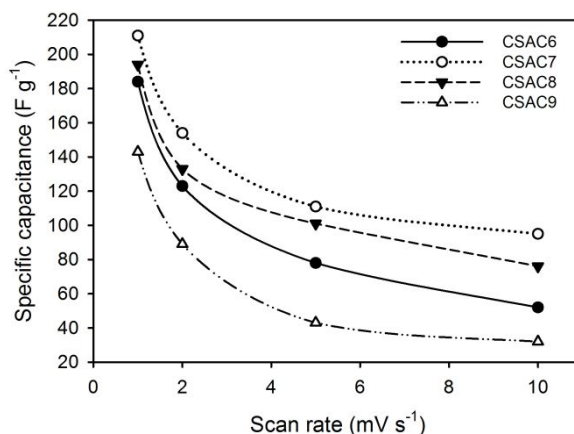


**Figure 6.** The curve of specific capacitance vs. scan rate of CSAC6, CSAC7, CSAC8, and CSAC9

The specific capacitances of CSAC6, CSAC7, CSAC8, and CSAC9 were also evaluated at different scan rates from  $1 \text{ mV s}^{-1}$  to  $10 \text{ mV s}^{-1}$ , as shown in Figure 6. The activated carbon which maintained the highest specific capacitance of 45% was CSAC7, followed by CSAC8, CSAC6, and CSAC9 with values of 39%, 28%, and 23%, respectively. The galvanostatic charge-discharge (GCD) curves of symmetric cells CSAC6, CSAC7, CSAC8, and CSAC9 at a current density of  $1 \text{ A g}^{-1}$  are shown in Figure 7a. In general, the GCD curve displays a normal profile for the EDLC type with a slightly faint  $iR$  drop. According to the GCD profile, the specific capacitances produced at CSAC6, CSAC7, CSAC8, and CSAC9 were 152, 237, 174 and  $124 \text{ F g}^{-1}$ , respectively, in the electrolyte of  $1 \text{ M H}_2\text{SO}_4$ . Higher activation temperature from  $600^\circ\text{C}$  to  $700^\circ\text{C}$  confirmed micro-mesopores combinations of 48.41% and 51.59% displayed the highest electrochemical properties from  $152 \text{ F g}^{-1}$  to  $237 \text{ F g}^{-1}$ . These results correlate with SEM,  $\text{N}_2$  gas adsorption/desorption, and CV analysis. The high activation temperature of from  $700^\circ\text{C}$  to  $900^\circ\text{C}$  decreased the capacitive value of the carbon



electrode up to  $124 \text{ F g}^{-1}$  for the CSAC9 sample. This is associated with the collapse of the pore walls and the erosion of the carbon framework structure to cover the active site of the ionic charge below [37].

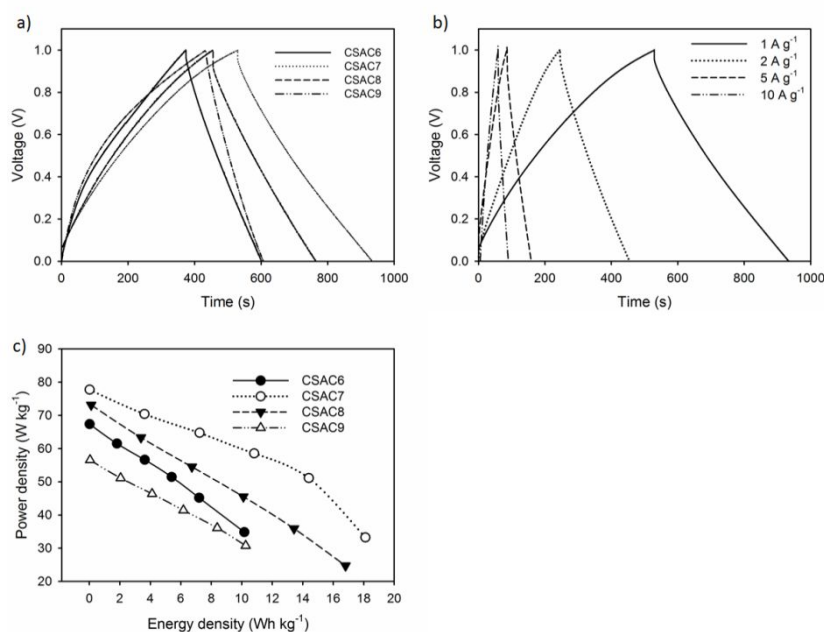


**Figure 7.** (a) GCD curve of CSAC6, CSAC7, CSAC8, and CSAC9, (b) GCD curve at different current density of CSAC7, and (c) Ragone plot of CSAC6, CSAC7, CSAC8, and CSAC9 in  $1 \text{ M H}_2\text{SO}_4$  electrolyte

Furthermore, the resistance in CSAC7 was lower at  $0.0025 \Omega$  due to the relatively high dominance of the mesopores which improved the diffusion of ionic charges in all directions compared to CSAC6, CSAC8, and CSAC9 which has a higher resistance value of  $0.012$ ,  $0.27$ , and  $0.034 \Omega$ , respectively. In addition, the GCD profile of CSAC7 was reviewed at different current density of  $1$ ,  $2$ ,  $5$ , and  $10 \text{ A g}^{-1}$ , as shown in Figure 7b. It can be noted that the GCD curves of CSAC7 still maintain primary symmetric triangle shape at  $10 \text{ A g}^{-1}$  suggesting stable double-layer capacitor behaviors, fast ion response, and low internal resistance in EDL processes<sup>42</sup>. At  $1 \text{ A g}^{-1}$ , CSAC7 sample delivers a specific capacitance of  $237 \text{ F g}^{-1}$  and it still maintains  $210 \text{ F g}^{-1}$  at  $10 \text{ A g}^{-1}$ , initiating a high-rate performance of  $88.6\%$ . To compare the performance of both samples in-depth, Ragone plots were used to

evaluate the energy and power density which are calculated using standard formulas as shown in Figure 7c. Symmetrical supercapacitors CSAC6, CSAC7, CSAC8 and CSAC9 assembled with an aqueous electrolyte of 1M H<sub>2</sub>SO<sub>4</sub> in an organic separator had energy densities of 10.1712, 18.1081, 16.8049 and 10.2596 Wh kg<sup>-1</sup> as well as power densities of 67.3793, 77.74, 73.1373 and 56.5421 W kg<sup>-1</sup>, respectively. The high electrochemical capability of CSAC7 is due to the 3D hierarchical porous structure and the specific surface area which provides a short and accessible ion transfer area in all directions for ionic charges to diffuse at the electrode/electrolyte interface.

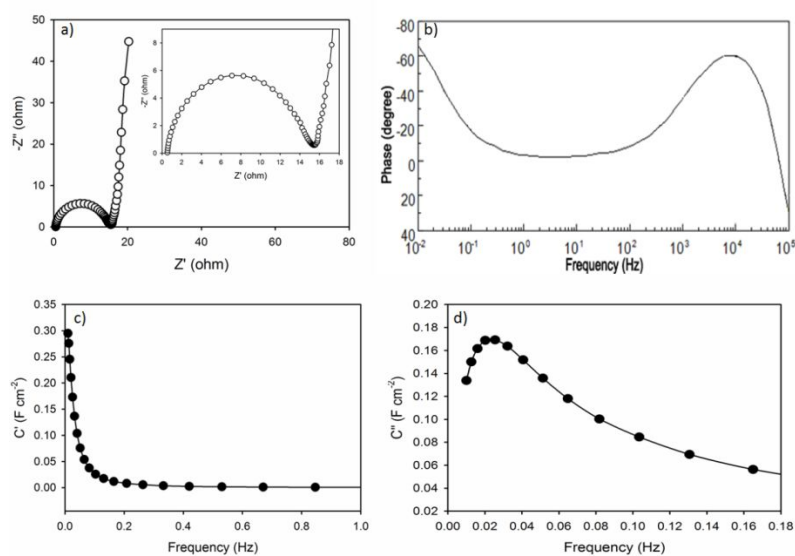


**Figure 8.** (a) Nyquist plot, (b) Bode phase angle plot, (c) real capacitance ( $C'$ ) vs. frequency plot, and (d) imaginer capacitance ( $C''$ ) vs. frequency plot of CSAC7 symmetrical devices

The high electrochemical confirmation of CSAC7 was reviewed in depth via a Nyquist Plot with a limited diffusion area in the frequency range of 0.01 Hz to 100,000 Hz, as shown in Figure 8a. Horizontal translation along the  $Z'$  axis confirms a relatively low  $R_s$  0.87  $\Omega\text{cm}^2$  indicating a good ions adsorption and desorption process at the electrode-electrolyte interface. Furthermore, the RCT (12.3  $\Omega\text{cm}^2$ ) interpreted at the semicircular position confirmed the fast charge transfer kinetically as a result of the current passing through the

1  
2  
3 electrode forming an electric layer. This is due to the hierarchical pores structure with a  
4 combination of micro, meso, and macropores initiates the active site which is followed by the  
5 ability of ion diffusion in all directions without any obstacles. In addition, the straight line  
6 that tends to be perpendicular at low frequencies confirms the pure capacitive and high ion  
7 transfer rate at the CSAC7 electrode. The Bode phase angle plot of CSAC7 was also  
8 evaluated as shown in Figure 8b. The phase angle at low frequencies reveals specific  
9 information about the ability of the electrode to generate an electric double layer. CSAC7  
10 electrode displays a phase angle close to  $-90^\circ$  indicating that the normal dielectric layer of the  
11 EDLC version is accompanied by impaired ion degradation due to self-heteroatom doping. In  
12 addition, the Bode phase angle plot provides further information for the characteristics of the  
13 conductive material through analysis of the real capacitance ( $C'$ ) and the imaginary  
14 capacitance ( $C''$ ) with respect to frequency, as shown in Figures 8b, and 8c. The  $C'$  values are  
15 weak in the lower frequency and higher frequency regions, the  $C'$  values show less frequency  
16 dependence, indicating a purely resistive behavior in CSAC7. Moreover, the value of the  
17 imaginary capacitance  $C''$  at the peak frequency confirms a relaxation time of 9.25 seconds,  
18 indicating that the symmetrical CSAC7 device acts as a pure capacitor. This value indicates a  
19 measure of how quickly the stored energy of the device can be efficiently distributed. For  
20 comparison, the obtained carbon nanofiber-based on corn silk waste showed higher  
21 electrochemical properties than the carbon nanofiber-based on bacterial cellulose and tofu  
22 dregs obtained through chemical activation of KOH and  $H_3PO_4$  [40,43]. In addition, although  
23 polymer-based carbon nanofibers exhibit superior specific capacitance, our study was able to  
24 produce higher energy densities than the previously reported as confirmed in referee [42].  
25 This is due to the combination of nanofiber and micro-mesoporous structures allowing the  
26 provision of high active sites and ion-transport channels. Moreover, the binder-free electrode  
27 design supports the high electrochemical performance of the supercapacitor.  
28  
29  
30  
31  
32  
33  
34  
35  
36  
37  
38  
39  
40  
41  
42  
43  
44  
45  
46  
47  
48  
49  
50  
51  
52  
53  
54  
55  
56  
57  
58  
59  
60

#### 4. Conclusion

Based on the results, hierarchically porous carbon nanofiber was successfully obtained from corn silk using a low-cost, simple, and sustainable technique without a binding material for a high energy density of symmetric supercapacitors. KOH activation using one-step integrated pyrolysis possessed excellent material properties including framework structure, porosity, wettability, and amorphousibility. Furthermore, different physical activation temperatures display distinctive pores structure with individual advantages. At 700 °C, a 3D hierarchical pore structure was displayed followed by a high surface area leading to the formation of an ideal combination of micro and mesopores for enhancing the high performance of the electrode material. Using a two-electrode binder-free system, CSAC7 showed the best electrochemical properties with a specific capacitance of 237 F g<sup>-1</sup> in a 1 M H<sub>2</sub>SO<sub>4</sub> aqueous electrolyte. Hence, the maximum energy density of 18.19 Wh kg<sup>-1</sup> and power density of 77.74 W kg<sup>-1</sup> at current density of 1 A g<sup>-1</sup>. This result shows that the approach applied in this study confirmed the potential of corn silk as an activated carbon based material with high properties.

#### Acknowledgement

This study was funded by the collaborative grants between universities, State Islamic University of Sultan Syarif Kasim Riau with contract No. 873/Un.04/L. 1/TL.01/03/2022.

#### References

- [1] Poonam, Sharma K, Arora A and Tripathi S K 2019 Review of supercapacitors: Materials and devices *J. Energy Storage* **21** 801–25
- [2] Kumar R, Sahoo S, Joanni E, Singh R K, Tan W K, Kar K K and Matsuda A 2019 Recent progress in the synthesis of graphene and derived materials for next generation electrodes of high performance lithium ion batteries *Prog. Energy Combust. Sci.* **75** 100786
- [3] Chen T and Dai L 2013 Carbon nanomaterials for high-performance supercapacitors *Mater. Today* **16** 272–80
- [4] Zhai Y, Dou Y, Zhao D, Fulvio P F, Mayes R T and Dai S 2011 Carbon Materials for Chemical Capacitive Energy Storage *Adv. Mater.* **23** 4828–50
- [5] Taer E and Taslim R 2018 Brief Review: Preparation Techniques of Biomass Based Activated Carbon Monolith Electrode for Supercapacitor Applications *AIP Conference*

- 1  
2  
3 *Proceedings* vol 1927 pp 020004-1-020004-4
- 4 [6] Miller E E, Hua Y and Tezel F H 2018 Materials for energy storage: Review of  
5 electrode materials and methods of increasing capacitance for supercapacitors *J.*  
6 *Energy Storage* **20** 30–40
- 7 [7] Tiwari S K, Sahoo S, Wang N and Huczko A 2020 Graphene research and their  
8 outputs: Status and prospect *J. Sci. Adv. Mater. Devices* **5** 10–29
- 9 [8] Mensah-Darkwa K, Zequine C, Kahol P K and Gupta R K 2019 Supercapacitor  
10 energy storage device using biowastes: A sustainable approach to green energy  
11 *Sustain.* **11**
- 12 [9] Bhat V S, Kanagavalli P, Sriram G, B R P, John N S, Veerapandian M, Kurkuri M  
13 and Hegde G 2020 Low cost, catalyst free, high performance supercapacitors based on  
14 porous nano carbon derived from agriculture waste *J. Energy Storage* **32** 101829
- 15 [10] Fu Y, Zhang N, Shen Y, Ge X and Chen M 2018 Micro-mesoporous carbons from  
16 original and pelletized rice husk via one- step catalytic pyrolysis *Bioresour. Technol.*  
17 **269** 67–73
- 18 [11] Su X, Li S, Jiang S, Peng Z, Guan X and Zheng X 2018 Superior capacitive behavior  
19 of porous activated carbon tubes derived from biomass waste-cotonier strobili fibers  
20 *Adv. Powder Technol.* **29** 2097–107
- 21 [12] Tan H, Tang J, Kim J, Kaneti Y V, Kang Y M, Sugahara Y and Yamauchi Y 2019  
22 Rational design and construction of nanoporous iron- and nitrogen-doped carbon  
23 electrocatalysts for oxygen reduction reaction *J. Mater. Chem. A* **7** 1380–93
- 24 [13] Yin L, Chen Y, Li D, Zhao X, Hou B and Cao B 2016 3-Dimensional hierarchical  
25 porous activated carbon derived from coconut fibers with high-rate performance for  
26 symmetric supercapacitors *Mater. Des.* **111** 44–50
- 27 [14] Wan L, Chen D, Liu J, Zhang Y, Chen J, Du C and Xie M 2020 Facile preparation of  
28 porous carbons derived from orange peel via basic copper carbonate activation for  
29 supercapacitors *J. Alloys Compd.* **823** 153747
- 30 [15] Sodtipinta J, Ieosakulrat C, Poonyayant N, Kidkhunthod P, Chanlek N, Amornsakchai  
31 T and Pakawatpanurut P 2017 Interconnected open-channel carbon nanosheets derived  
32 from pineapple leaf fiber as a sustainable active material for supercapacitors *Ind.*  
33 *Crops Prod.* **104** 13–20
- 34 [16] Chen Z, Wang X, Xue B, Li W, Ding Z, Yang X, Qiu J and Wang Z 2020 Rice husk-  
35 based hierarchical porous carbon for high performance supercapacitors : The structure-  
36 performance relationship *Carbon N. Y.* **161** 432–44
- 37 [17] Liangshuo L, Lin Q, Xinyu L, Ming D and Xin F 2020 Preparation of biomass-based  
38 porous carbon derived from waste ginger slices and its electrochemical performance  
39 *Optoelectron. Adv. Mater. Rapid Commun.* **14** 548–55
- 40 [18] He X, Li R, Han J, Yu M and Wu M 2013 Facile preparation of mesoporous carbons  
41 for supercapacitors by one-step microwave-assisted ZnCl<sub>2</sub> activation *Mater. Lett.* **94**  
42 158–60
- 43 [19] Taer E, Pratiwi L, Apriwandi, Mustika W S, Taslim R and Agustino 2020 Three-  
44 dimensional pore structure of activated carbon monolithic derived from hierarchically  
45 bamboo stem for supercapacitor application *Commun. Sci. Technol.* **5** 22–30
- 46 [20] Yang V, Senthil R A, Pan J, Kumar T R, Sun Y and Liu X 2020 Hierarchical porous  
47 carbon derived from jujube fruits as sustainable and ultrahigh capacitance material for  
48 advanced supercapacitors *J. Colloid Interface Sci.* **579** 347–56
- 49 [21] Jiang X, Guo F, Jia X, Zhan Y, Zhou H and Qian L 2020 Synthesis of nitrogen-doped  
50 hierarchical porous carbons from peanut shell as a promising electrode material for  
51 high-performance supercapacitors *J. Energy Storage* **30** 101451
- 52 [22] Shang Z, An X, Liu L, Yang J, Zhang W, Dai H, Cao H, Xu Q, Liu H and Ni Y 2021

- Chitin nanofibers as versatile bio-templates of zeolitic imidazolate frameworks for N-doped hierarchically porous carbon electrodes for supercapacitor *Carbohydr. Polym.* **251** 117107
- [23] Men B, Guo P, Sun Y, Tang Y, Chen Y, Pan J and Wan P 2019 High-performance nitrogen-doped hierarchical porous carbon derived from cauliflower for advanced supercapacitors *J. Mater. Sci.* **54** 2446–57
- [24] Mitravinda T, Nanaji K, Anandan S, Jyothirmayi A, Chakravadhanula V S K, Sharma C S and Rao T N 2018 Facile Synthesis of Corn Silk Derived Nanoporous Carbon for an Improved Supercapacitor Performance *J. Electrochem. Soc.* **165** A3369–79
- [25] Zhou J, Yuan S, Lu C, Yang M and Song Y 2020 Hierarchical porous carbon microtubes derived from corn silks for supercapacitors electrode materials *J. Electroanal. Chem.* **878** 114704
- [26] Girgis B S, Temerk Y M, Gadelrab M M and Abdullah I D 2007 X-ray Diffraction Patterns of Activated Carbons Prepared under Various Conditions *Carbon Sci.* **8** 95–100
- [27] Serafin J, Baca M, Biegun M, Mijowska E, Kaleńczuk R J, Sreńscek-Nazzal J and Michalkiewicz B 2019 Direct conversion of biomass to nanoporous activated biocarbons for high CO<sub>2</sub> adsorption and supercapacitor applications *Appl. Surf. Sci.* **497** 143722
- [28] Márquez-Montesino F, Torres-Figueroa N, Lemus-Santana A and Trejo F 2020 Activated Carbon by Potassium Carbonate Activation from Pine Sawdust (*Pinus montezumae* Lamb.) *Chem. Eng. Technol.* **43** 1716–25
- [29] Taer E, Apriwandi A, Taslim R, Agutino A and Yusra D A 2020 Conversion *Syzygium oleana* leaves biomass waste to porous activated carbon nanosheet for boosting supercapacitor performances *J. Mater. Res. Technol.* **9** 13332–40
- [30] Gou G, Huang F, Jiang M, Li J and Zhou Z 2020 Hierarchical porous carbon electrode materials for supercapacitor developed from wheat straw cellulosic foam *Renew. Energy* **149** 208–16
- [31] Jiang W, Pan J and Liu X 2019 A novel rod-like porous carbon with ordered hierarchical pore structure prepared from Al-based metal-organic framework without template as greatly enhanced performance for supercapacitor *J. Power Sources* **409** 13–23
- [32] Taer E, Apriwandi, Dalimunthe B K L and Taslim R 2021 A rod-like mesoporous carbon derived from agro-industrial cassava petiole waste for supercapacitor application *J. Chem. Technol. Biotechnol.* **96** 662–71
- [33] Taer E, Apriwandi A, Agutino A, Taslim R, Mustika W S and Exa Fadli 2021 Surface modification: unique ellipsoidal/strobili-fiber structure of porous carbon monolith for electrode supercapacitor *Nanosci. Technol. An Int. J.* **12** 45–63
- [34] Duan B, Gao X, Yao X, Fang Y, Huang L, Zhou J and Zhang L 2016 Unique elastic N-doped carbon nanofibrous microspheres with hierarchical porosity derived from renewable chitin for high rate supercapacitors *Nano Energy* **27** 482–91
- [35] Liu F, Wang Z, Zhang H, Jin L, Chu X, Gu B, Huang H and Yang W 2019 Nitrogen, oxygen and sulfur co-doped hierarchical porous carbons toward high-performance supercapacitors by direct pyrolysis of kraft lignin *Carbon N. Y.* **149** 105–16
- [36] Abioye A M and Ani F N 2015 Recent development in the production of activated carbon electrodes from agricultural waste biomass for supercapacitors: A review *Renew. Sustain. Energy Rev.* **52** 1282–93
- [37] Ayinla R T, Dennis J O, Zaid H M, Sanusi Y K, Usman F and Adebayo L L 2019 A review of technical advances of recent palm bio-waste conversion to activated carbon for energy storage *J. Clean. Prod.* **229** 1427–42.



Rika Taslim &lt;rikataslim@gmail.com&gt;

**[ANSN-2022-0119] - Decision on Manuscript: MAJOR REVISION**

1 message

**NQL Editor-in-Chief** <onbehalf@manuscriptcentral.com>

Sat, Aug 6, 2022 at 8:17 PM

Reply-To: ansn.eic@vast.vn

To: rikataslim@gmail.com

06-Aug-2022

Dear Dr. Taslim:

Manuscript ID ANSN-2022-0119 entitled "Agricultural Bio-waste-derived Hierarchical Porous Carbon Nanofiber for High-performance Supercapacitors" which you submitted to the Advances in Natural Sciences: Nanoscience and Nanotechnology (ANSN), has been reviewed. The comments of the Associate Editor and Reviewers are included at the bottom of this letter.

The Reviewers have recommended publication, but also suggest some revisions to your manuscript. Therefore, I invite you to respond to the Reviewers' comments and revise your manuscript accordingly.

To revise your manuscript, log into <https://mc04.manuscriptcentral.com/vastansn> and enter your Author Center, where you will find your manuscript title listed under "Manuscripts with Decisions". Under "Actions", click on "Create a Revision". Your manuscript number has been appended to denote a revision.

You may also click the below link to start the revision process (or continue the process if you have already started your revision) for your manuscript. If you use the below link you will not be required to login to ScholarOne Manuscripts.

\*\*\* PLEASE NOTE: This is a two-step process. After clicking on the link, you will be directed to a webpage to confirm. \*\*\*

[https://mc04.manuscriptcentral.com/vastansn?URL\\_MASK=c1a3a7f73bc34e598fc8cad0124f2f9e](https://mc04.manuscriptcentral.com/vastansn?URL_MASK=c1a3a7f73bc34e598fc8cad0124f2f9e)

You will be unable to make your revisions on the originally submitted version of the manuscript. Instead, revise your manuscript using a word processing program and save it on your computer. Please also highlight the changes to your manuscript within the document by using the track changes mode in MS Word or by using bold or colored text.

Once the revised manuscript is prepared using ANSN's template which could be downloaded via URL: [https://mc04.manuscriptcentral.com/societyimages/vastansn/ANSN\\_Template.zip](https://mc04.manuscriptcentral.com/societyimages/vastansn/ANSN_Template.zip), you can upload it and submit it through your Author Center.

When submitting your revised manuscript, you will be able to respond to the comments made by the reviewers in the space provided. You can use this space to document any changes you make to the original manuscript. In order to expedite the processing of the revised manuscript, please be as specific as possible in your response to the reviewers.

**IMPORTANT:** Your original files are available to you when you upload your revised manuscript. Please delete any redundant files before completing the submission.

Because we are trying to facilitate timely publication of manuscripts submitted to the Advances in Natural Sciences: Nanoscience and Nanotechnology, your revised manuscript should be submitted by 05-Sep-2022. If it is not possible for you to submit your revision by this date, we may have to consider your paper as a new submission. Please inform us at [journal@ans.vast.vn](mailto:journal@ans.vast.vn) if you need an extension in order to revise this paper.

Once again, thank you for submitting your manuscript to the Advances in Natural Sciences: Nanoscience and Nanotechnology and I look forward to receiving your revision.

Sincerely,

Editor-in-Chief  
Advances in Natural Sciences: Nanoscience and Nanotechnology  
Jointly published by VAST (VN) and IOP (UK)  
Abstracted in Web of Science (ESCI), Scopus, Chemical Abstracts,...  
E-mail: [journal@ans.vast.vn](mailto:journal@ans.vast.vn)

Homepage: <https://iopscience.iop.org/ansn>; <https://ans.vast.vn/>  
 Manuscript submission: <https://mc04.manuscriptcentral.com/vastansn>

---

Associate Editor's comments:

- The numbers of the tables must be corrected.
- XRD patterns should be changed by the better ones.
- There is a discrepancy between the citation in text and the list of references, please double-check.
- The manuscript is quite long. Please shorten it, remove the redundant writing. Note that a regular article (including all text and figures/tables) should not be longer than 10 journal pages.
- Some relevant articles below could be considered:

<https://doi.org/10.1088/2043-6262/ac5dc8>  
<https://doi.org/10.1088/2043-6262/abffca>  
<https://doi.org/10.1088/2043-6262/abe93e>  
<https://doi.org/10.1149/MA2020-01271893mtgabs>

However, total number of the references in a regular article published in the ANSN should be less than 40. Therefore, only reasonably appropriate references should be selected.

---

Reviewers' Comments to Author:

Reviewer: 1

Comments to the Author

The authors here prepared a kind of biomass-derived carbon (biocarbon) [Ref. 1-2] and studied its application in EDLC. The method and application here referred to are routine, however, the carbon precursor (corn silk) and the activation agent (KOH/CO<sub>2</sub> compared to single KOH) as well as the eggshell inner membrane separator is relatively new and of some interest [Ref. 3-9], which may add a member into the biocarbon family for EDLC application. Thus, after addressing the following concerns it may be published in the Journal.

- 1) The title may be improved to be specific by including the carbon precursor "corn silk", and the claimed "Hierarchical Porous Carbon Nanofiber" may not be verified by the characterizations, please consider improvement/alteration.
- 2) About the "duck eggshell membrane", please give some content on the advantages of this kind of separator. (<https://www.exploratorium.edu/cooking/eggs/eggcomposition.html>)
- 3) It is depicted that "dried corn silks powder was dissolved with a 0.5 m/L KOH solution," "The sample was precipitated and dried," is it more appropriate if replaced by "dispersed" rather than "dissolved", and by "precipitated and filtered", please specify it.
- 4) The structures in Fig 2 by SEM seem broken and powdered, any reasons? And why are there some nanofibers in the biocarbon, e.g., Fig 2h, please further discuss it?
- 5) Why the corn silk calcinated at 700 oC showed the highest capacitance (Fig. 7), please give some further explanations.
- 6) Cycling performance (and coulombic efficiency) of the EDLC may be provided for better understanding, e.g., in Fig 7.
- 7) Some grammatical and format issues, e.g., "15Kv", "002 reflection plane", "100 reflection plane", "P/P0>0.9".
- 8) Some more related references may be cited for better understanding.

Ref.

1. Resol-Vegetable Fibers Composites, Materials Research Foundations, Vol. 122, pp 154-198, 2022. DOI: <https://doi.org/10.21741/9781644901854-7>
  2. J. Vac. Sci. Technol. A 2019, 37, 040803. <https://avs.scitation.org/doi/abs/10.1116/1.5095413>
  3. Hierarchical porous carbon microtubes derived from corn silks for supercapacitors electrode materials, Journal of Electroanalytical Chemistry 878 (2020) 114704.
  4. Mater. Today Energy 2017, 5, 196-204. <https://doi.org/10.1016/j.mtener.2017.06.011>
  5. Bio-waste wood-derived porous activated carbon with tuned microporosity for high performance supercapacitors, Journal of Energy Storage, Volume 52, Part B, 15 August 2022, 104928
  6. Preparation of porous agro-waste-derived carbon from onion peel for supercapacitor application. J Mater Sci 55, 4213–4224 (2020). <https://doi.org/10.1007/s10853-019-04236-7>
  7. Hierarchical porous activated carbon for supercapacitor derived from corn stalk core by potassium hydroxide activation, Electrochimica Acta, Volume 212, 10 September 2016, Pages 839-847.
  8. Effect of TiO<sub>2</sub> on Duck Eggshell Membrane as Separators in Supercapacitor Applications, Materials Science Forum (Volume 827), 2015, 51-155. <https://doi.org/10.4028/www.scientific.net/MSF.827.151>
- 

Reviewer: 2

Comments to the Author

In this paper, the author has obtained hierarchically porous carbon nanofiber successfully from corn silk using a low-cost, simple, and sustainable technique without a binding material for a high energy density of symmetric supercapacitors. When the pyrolysis temperature was 700 oC, a 3D hierarchical pore structure was displayed followed by a high surface area leading to the formation of an ideal combination of micro and mesopores for



enhancing the high performance of the electrode material. What's more, CSAC7 showed the best electrochemical properties with a specific capacitance of 237 F g<sup>-1</sup> in a 1 M H<sub>2</sub>SO<sub>4</sub> aqueous electrolyte. I would like to recommend it for publication after minor revisions. The detailed comments are as follows:

1. Since the material studied is porous carbon nanofiber, Raman characterization is necessary. Please add relevant characterization.
  2. Please add the XRD spectrum of CSAC6 and CSAC8.
  3. The descriptions of Fig. 3b and Fig. 3c appear in the paper, but relevant figures are missing. Please add these figures.
  4. Please check the whole manuscript carefully, for example, the "physical activation at a higher temperature above 700 °C led to a better decomposition into the basic components including hemicellulose, cellulose, lignin compared to 600oC" on page 7 should be changed to "physical activation at a higher temperature above 700 °C led to a better decomposition into the basic components including hemicellulose, cellulose, lignin compared to 600 oC".
  5. Some important papers should be cited in this paper:  
Natl. Sci. Rev., 2020, 7, 305-314.  
Small Methods, 2021, doi: 10.1002/smt.202101070.  
Angew. Chem. Int. Ed., 2021, 60, 25318.  
EnergyChem, 2019, 1, 100016.
- 

Reviewer: 3

#### Comments to the Author

This is an interesting article and worth publishable in *Advances in Natural Sciences: Nanoscience and Nanotechnology*. However, I suggest a revision addressing following queries prior to consideration for publication.

1. Four samples were obtained but only two samples were evaluated, where are the others samples?
  2. Why physical activation and chemical activation were used simultaneously? As you know, only chemical activation can also give a large BET surface area, I can't find any necessary explanation.
  3. The role of physical activation and chemical activation should be enhanced.
  4. In Figure 2, only a few amount of Nanofiber were observed, i.e., morphology of samples is mainly irregular granular not the Nanofiber, so the title should be modified.
  5. What is the mass loading in an electrode?
  6. More structural characterization, like XPS, Raman, (HR)TEM etc are required to understand the better electrochemical performance.
  7. The energy densities have been overestimated significantly. For example, for a supercapacitor device with the cell voltage is 3.0 V, the specific capacitance is 200 F/g (the corresponding cell capacitance is 50 F/g), the energy density is calculated to be 62.5 Wh/kg. For your device, however, the energy density can reach to 316.77 Wh/kg with a narrow working potential window of 1 V. It seems the unit was not converted.
  8. I recommend the authors to refer others reported electrode materials in aqueous/nonaqueous electrolyte especially in the last three years.
  9. The use of porous carbon materials for energy devices represents a topic highly in vogue nowadays, these relevant publications in the field are worth to be discussed: *Electrochimica Acta* 379 (2021) 138170; *Carbon* 141 (2019) 40-49.
- 

Reviewer: 4

#### Comments to the Author

The analyse for the structure-activity relationship is the key in the manuscript, however, only the samples at 700 and 900 °C were characterized, which is inadequate. Therefore, the samples at 600 and 800 °C should be characterized. In addition, the chemical environment on the surface of as-prepared carbon is very important for the capacitance properties, therefore, the FTIR or XPS analyse should be provided in this manuscript. Finally, the TEM images of carbon should be provided to observe the porous structure. In conclusion, I recommend that the manuscript can not be considered because of the obvious defect in the characterization.



Rika Taslim <rikataslim@gmail.com>

---

## [ANSN-2022-0119.R1] - Manuscript Submitted

1 message

---

**NVT Secretariat of ANSN** <onbehalf@manuscriptcentral.com>

Mon, Aug 15, 2022 at 11:35 AM

Reply-To: journal@ans.vast.vn

To: rikataslim@gmail.com

15-Aug-2022

Dear Dr. Taslim:

Your manuscript entitled "Agricultural Bio-waste of Corn Silk derived Porous Carbon for High-performance Supercapacitors" has been successfully submitted online and is presently being given full consideration for publication in the Advances in Natural Sciences: Nanoscience and Nanotechnology (ANSN).

Your manuscript ID is ANSN-2022-0119.R1.

Please mention the above manuscript ID in all future correspondence or when calling the office for questions. If there are any changes in your street address or e-mail address, please log in to ScholarOne Manuscripts at <https://mc04.manuscriptcentral.com/vastansn> and edit your user information as appropriate.

You can also view the status of your manuscript at any time by checking your Author Center after logging in to <https://mc04.manuscriptcentral.com/vastansn>.

Thank you for submitting your manuscript to the Advances in Natural Sciences: Nanoscience and Nanotechnology. If you have any questions, feel free to contact us at [journal@ans.vast.vn](mailto:journal@ans.vast.vn).

Sincerely,

Editorial Office

Advances in Natural Sciences: Nanoscience and Nanotechnology (ANSN)

Jointly published by VAST (VN) and IOP (UK)

Abstracted in Web of Science (ESCI), Scopus, Chemical Abstracts,...

E-mail: [journal@ans.vast.vn](mailto:journal@ans.vast.vn)

Homepage: <https://iopscience.iop.org/ansn>; <https://ans.vast.vn/>

Manuscript submission: <https://mc04.manuscriptcentral.com/vastansn>



Rika Taslim &lt;rikataslim@gmail.com&gt;

---

**[ANSN-2022-0119.R1] - Manuscript Submitted**

1 message

---

**NVT Secretariat of ANSN** <onbehalf@manuscriptcentral.com>  
Reply-To: journal@ans.vast.vn  
To: rikataslim@gmail.com

Mon, Aug 15, 2022 at 11:35 AM

15-Aug-2022

Dear Dr. Taslim:

Your manuscript entitled "Agricultural Bio-waste of Corn Silk derived Porous Carbon for High-performance Supercapacitors" has been successfully submitted online and is presently being given full consideration for publication in the Advances in Natural Sciences: Nanoscience and Nanotechnology (ANSN).

Your manuscript ID is ANSN-2022-0119.R1.

Please mention the above manuscript ID in all future correspondence or when calling the office for questions. If there are any changes in your street address or e-mail address, please log in to ScholarOne Manuscripts at <https://mc04.manuscriptcentral.com/vastansn> and edit your user information as appropriate.

You can also view the status of your manuscript at any time by checking your Author Center after logging in to <https://mc04.manuscriptcentral.com/vastansn>.

Thank you for submitting your manuscript to the Advances in Natural Sciences: Nanoscience and Nanotechnology. If you have any questions, feel free to contact us at [journal@ans.vast.vn](mailto:journal@ans.vast.vn).

Sincerely,

Editorial Office

Advances in Natural Sciences: Nanoscience and Nanotechnology (ANSN)

Jointly published by VAST (VN) and IOP (UK)

Abstracted in Web of Science (ESCI), Scopus, Chemical Abstracts,...

E-mail: [journal@ans.vast.vn](mailto:journal@ans.vast.vn)Homepage: <https://iopscience.iop.org/ansn>; <https://ans.vast.vn/>Manuscript submission: <https://mc04.manuscriptcentral.com/vastansn>



Rika Taslim &lt;rikataslim@gmail.com&gt;

**[ANSN-2022-0119.R1] -**

3 messages

**Thanh Tran Dang** <onbehalf@manuscriptcentral.com>  
Reply-To: thanhtd@ims.vast.ac.vn  
To: rikataslim@gmail.com

Tue, Sep 6, 2022 at 5:05 PM

06-Sep-2022

ANSN-2022-0119.R1 - Agricultural Bio-waste of Corn Silk derived Porous Carbon for High-performance Supercapacitors

Dear Dr. Rika Taslim:

Your manuscript, referenced above, has been reviewed for publication in the ANSN:  
Comments from the reviewer(s) are included below.  
We conclude that further review and revision may be necessary.

Reviewer 1 has recommended that your manuscript must be minor revised.  
We request that you for carefully revising the manuscript. Then, send the revised manuscript with revisions highlighted along with the Response letter to the reviewer via email to us for further consideration by 13-Sept-2022.

If you have any questions, please feel free to contact us at [thanhtd@ims.vast.ac.vn](mailto:thanhtd@ims.vast.ac.vn) and/or [journal@ans.vast.vn](mailto:journal@ans.vast.vn).  
We are looking forwards to hearing from you.

Thanks and regards

-----  
Reviewer 1.

Comments to the author:

The manuscript improved a lot after modification according to the suggestions, it is now recommended for publication.  
Some tiny format issues, such as Ref. 31, and the significant digits (pore holes structure in the 64-7214 nm range).

-----  
Sincerely,

Prof. Thanh Tran Dang  
[thanhtd@ims.vast.ac.vn](mailto:thanhtd@ims.vast.ac.vn)

Advances in Natural Sciences: Nanoscience and Nanotechnology (ANSN)  
Jointly published by VAST (VN) and IOP (UK)  
Abstracted in Web of Science (ESCI), Scopus, Chemical Abstracts,...  
E-mail: [journal@ans.vast.vn](mailto:journal@ans.vast.vn)  
Homepage: <https://iopscience.iop.org/ansn>; <https://ans.vast.vn/>  
Manuscript submission: <https://mc04.manuscriptcentral.com/vastansn>

**Thanh Tran Dang** <onbehalf@manuscriptcentral.com>  
Reply-To: thanhtd@ims.vast.ac.vn  
To: rikataslim@gmail.com

Tue, Sep 6, 2022 at 5:05 PM

06-Sep-2022

ANSN-2022-0119.R1 - Agricultural Bio-waste of Corn Silk derived Porous Carbon for High-performance Supercapacitors

Dear Dr. Rika Taslim:

Your manuscript, referenced above, has been reviewed for publication in the ANSN:  
Comments from the reviewer(s) are included below.  
We conclude that further review and revision may be necessary.

Reviewer 1 has recommended that your manuscript must be minor revised.

We request that you for carefully revising the manuscript. Then, send the revised manuscript with revisions highlighted along with the Response letter to the reviewer via email to us for further consideration by 13-Sept-2022.

If you have any questions, please feel free to contact us at [thanhtd@ims.vast.ac.vn](mailto:thanhtd@ims.vast.ac.vn) and/or [journal@ans.vast.vn](mailto:journal@ans.vast.vn). We are looking forwards to hearing from you.

Thanks and regards

-----  
Reviewer 1.

Comments to the author:

The manuscript improved a lot after modification according to the suggestions, it is now recommended for publication. Some tiny format issues, such as Ref. 31, and the significant digits (pore holes structure in the 64-7214 nm range).

-----  
Sincerely,

Prof. Thanh Tran Dang  
[thanhtd@ims.vast.ac.vn](mailto:thanhtd@ims.vast.ac.vn)

Advances in Natural Sciences: Nanoscience and Nanotechnology (ANSN)  
Jointly published by VAST (VN) and IOP (UK)  
Abstracted in Web of Science (ESCI), Scopus, Chemical Abstracts,...  
E-mail: [journal@ans.vast.vn](mailto:journal@ans.vast.vn)  
Homepage: <https://iopscience.iop.org/ansn>; <https://ans.vast.vn/>  
Manuscript submission: <https://mc04.manuscriptcentral.com/vastansn>

---

**Rika Taslim** <[rikataslim@gmail.com](mailto:rikataslim@gmail.com)>  
To: [thanhtd@ims.vast.ac.vn](mailto:thanhtd@ims.vast.ac.vn)

Wed, Sep 7, 2022 at 9:45 AM

07-Sept-2022

ANSN-2022-0119.R1 - Agricultural Bio-waste of Corn Silk derived Porous Carbon for High-performance Supercapacitors

Dear Prof. Thanh Tran Dang

Thank you for evaluating our manuscript in *Advances in Natural Sciences: Nanoscience and Nanotechnology* (ANSN).

We greatly appreciate the editor's consideration of this manuscript for publication and valuable review comments. We have made every attempt to respond to all comments and questions raised by the reviewer and have adjusted the manuscript accordingly. All revisions in the manuscript are given a yellow highlight background.

Furthermore, we have added the revised manuscript and author response letter to reviewer in attachment file.

We confirm that this manuscript was revised in accordance with the reviewers' comments in *Advances in Natural Sciences: Nanoscience and Nanotechnology* (ANSN). We hope this manuscript can be accepted and published in the *Advances in Natural Sciences: Nanoscience and Nanotechnology* (ANSN).

Best regards,

Rika Taslim  
Corresponding Author

### Authors' Responses to Editors' Reviewers' Comments on the Manuscript

**Reviewer 1.**

Comments to the author:

The manuscript improved a lot after modification according to the suggestions, it is now recommended for publication. Some tiny format issues, such as Ref. 31, and the significant digits (pore holes structure in the 64-7214 nm range).

**Authors' Response:**

We appreciate and thank the reviewer for the very constructive comment in this manuscript. We apologize for the mistakes. Accordingly, we have corrected the format issues in ref 31 and we also corrected the significant digits in sentences "pore holes structure in the 64-7214 nm range" This revision has been added to the manuscript with yellow highlight background. Hopefully, the revised manuscript is found to be more convenient to read.

**Result and discussions part, page 8, with yellow highlight background**

... Figure 2c shows the relatively dominant pore holes structure in the 64-214 nm range. The diverse pore...

**References part, page 21, with yellow highlight background**

[31] Ni W, Shi L and Resol 2022 Vegetable Fibers Composites *Mat Res. Foundations* **122** 154-198

 [Manuscript Taslim et al ANSN \[revised\] 2nd.docx](#)

 [Respon author for reviewer ANSN 2nd.docx](#)

On Tue, Sep 6, 2022 at 5:05 PM Thanh Tran Dang <[onbehalf@manuscriptcentral.com](mailto:onbehalf@manuscriptcentral.com)> wrote:

06-Sep-2022

ANSN-2022-0119.R1 - Agricultural Bio-waste of Corn Silk derived Porous Carbon for High-performance Supercapacitors

Dear Dr. Rika Taslim:

Your manuscript, referenced above, has been reviewed for publication in the ANSN:

Comments from the reviewer(s) are included below.

We conclude that further review and revision may be necessary.

Reviewer 1 has recommended that your manuscript must be minor revised.

We request that you for carefully revising the manuscript. Then, send the revised manuscript with revisions highlighted along with the Response letter to the reviewer via email to us for further consideration by 13-Sept-2022.

If you have any questions, please feel free to contact us at [thanhtd@ims.vast.ac.vn](mailto:thanhtd@ims.vast.ac.vn) and/or [journal@ans.vast.vn](mailto:journal@ans.vast.vn).

We are looking forwards to hearing from you.

Thanks and regards

-----  
Reviewer 1.

Comments to the author:

The manuscript improved a lot after modification according to the suggestions, it is now recommended for publication. Some tiny format issues, such as Ref. 31, and the significant digits (pore holes structure in the 64-7214 nm range).

-----  
Sincerely,

Prof. Thanh Tran Dang  
[thanhtd@ims.vast.ac.vn](mailto:thanhtd@ims.vast.ac.vn)

Advances in Natural Sciences: Nanoscience and Nanotechnology (ANSN)

Jointly published by VAST (VN) and IOP (UK)

Abstracted in Web of Science (ESCI), Scopus, Chemical Abstracts,...

E-mail: [journal@ans.vast.vn](mailto:journal@ans.vast.vn)

Homepage: <https://iopscience.iop.org/ansn>; <https://ans.vast.vn/>

Manuscript submission: <https://mc04.manuscriptcentral.com/vastansn>



# ADVANCES IN NATURAL SCIENCES: NANOSCIENCE AND NANOTECHNOLOGY

## Agricultural Bio-waste of Corn Silk derived Porous Carbon for High-performance Supercapacitors

Journal:	<i>Advances in Natural Sciences: Nanoscience and Nanotechnology</i>
Manuscript ID	ANSN-2022-0119.R1
Manuscript Type:	Original Article
Date Submitted by the Author:	n/a
Complete List of Authors:	Taslim, Rika; State Islamic University Sultan Syarif Kasim, Department of Industrial Engineering Halbi, Suryandri; State Islamic University Sultan Syarif Kasim, Department of Industrial Engineering Apriwandi, Apriwandi; University of Riau - Binawidja Campus, Department of Physics Taer, Erman; University of Riau - Bina Widya Campus, Department of physics
Keywords:	Nanofiber, Porous carbon, electrode material, Supercapacitor
Classification numbers:	5.16, 5.18

SCHOLARONE™  
Manuscripts

## Agricultural Bio-waste of Corn Silk derived Porous Carbon for High-performance

### Supercapacitors

Rika Taslim<sup>1,\*</sup>, Suryandri Halbi<sup>1</sup>, Apriwandi Apriwandi<sup>2</sup>, Erman Taer<sup>2</sup>

<sup>1</sup> Department of Industrial Engineering, State Islamic University of Sultan Syarif Kasim, 28293 Simpang Baru, Riau, Indonesia

<sup>2</sup> Department of Physics, Faculty of Mathematics and Natural Sciences, University of Riau, 28293 Simpang Baru, Riau, Indonesia

Email: [rikataslim@gmail.com](mailto:rikataslim@gmail.com)

**Abstract.** This study aims to develop a novel, simple, efficient, and low-cost method to prepare hierarchical porous carbon nanofiber derived from corn silks (CSAC) through a one-step carbonization-physical activation process. The carbon precursors were activated by KOH solution at a high pyrolysis temperature to prepare activated porous carbon as an electrode material for supercapacitors without using binders. This study focused on the effect of different activation temperatures of 600, 700, 800, and 900°C on the production of highly porous carbon nanofiber. An enhancement mechanism is proposed, which not only performed high nanofiber structures to possess the large specific active surface area to enhance energy density but also achieve micro-mesopores combination to realize fast ion-transport channels for boosting high power density. A maximum specific surface area of approximately 1096.951 m<sup>2</sup> g<sup>-1</sup> was achieved by CSAC7. Furthermore, the electrochemical performance was evaluated using 1 M H<sub>2</sub>SO<sub>4</sub> solution as an electrolyte through a novel two-electrode binder-free system. The electrode materials produced a maximum specific capacitance of 237 F g<sup>-1</sup> at a current density of 1 A g<sup>-1</sup>. These excellent characteristics show that the synthetic approach has a great potential for fabricating high-performance supercapacitors.

Keywords: Nanofiber, porous carbon, electrode material, supercapacitor.

Classification numbers: 5.16, 5.18

### 1. Introduction

Supercapacitors are globally considered as superior storage devices due to the higher energy and power density compared to batteries, capacitors, and fuel cells [1]. In addition,



1  
2  
3 they function as suitable materials for electrical components, pulse laser systems, and other  
4 electronic devices [2]. Supercapacitors are also directly utilized or combined with batteries  
5 for certain electrical facilities, such as electric braking, starters, vehicle, and generators [3].  
6  
7 The electric double-layer capacitors (EDLC) are considered to be the best type due to the  
8 variable and adaptable active materials, low cost, abundant availability, superior material  
9 properties, maximum electrolyte flow rate, high operating temperature and conductivity,  
10 compatible with a variety of low and high current components, environmentally friendly, and  
11 relatively safer [4]. However, supercapacitors still have various challenges such as the  
12 relatively low energy compared to the high power density, expensive active materials, and  
13 complex synthetic methods. In different studies, the energy density of supercapacitors has  
14 been increased with various approaches, but with a reduced power density. The main key to  
15 improving the performance of supercapacitors is the active electrode material, followed by  
16 the electrolyte and separator [5]. Three groups of active electrode materials have been  
17 reported including conduction polymers, metal oxides, and carbon [6]. Conducting polymer  
18 materials and metal oxides were used to successfully increase the energy density up to 200  
19 Wh kg<sup>-1</sup> [7]. This is several times greater than the result from other studies in the last decade.  
20 However, both materials require complex, complicated, corrosive, and toxic instruments,  
21 hence, they are not recommended for environmentally friendly mass production. Therefore,  
22 activated carbon from biomass and bio-organic waste is more promising as it has superior and  
23 attractive characteristics including abundant availability, renewability, easy fabrication, and  
24 low cost [8,9]. Activated carbon materials also have a good performance in increasing and  
25 maintaining energy density, although the energy density produced is still relatively low  
26 compared to metal oxides and conduction polymers [10]. Additionally, biomass precursors  
27 rich in structurally diverse porosity and significant heteroatoms provide a large number of  
28 active ion contacts and facilitate the transport of electrolytic ion charges in various pores  
29  
30  
31  
32  
33  
34  
35  
36  
37  
38  
39  
40  
41  
42  
43  
44  
45  
46  
47  
48  
49  
50  
51  
52  
53  
54  
55  
56  
57  
58  
59  
60

1  
2  
3 including micro-, meso-, and macro- leading to a high performance of energy and balanced  
4 power density [11]. Moreover, the 3D hierarchical pore structure obtained from the biomass-  
5 derived activated carbon has been shown to increase the energy density up to 5 times coupled  
6 with a high power density [12]. Hierarchical porous carbon consisting of micro-, meso-, and  
7 macropores are obtained from various biomass precursors such as onion peel [13], pineapple  
8 leaves [14], rice husk [15], ginger waste [16], peanut shells [17], bamboo stem [18], and  
9 jujube fruit [19]. The peanut shell agricultural biomass produced activated carbon having a  
10 3D hierarchical pore structure as well as abundant micropores and mesopores with surface  
11 area=2014.6 m<sup>2</sup> g<sup>-1</sup>. Activated carbon is prepared by a new and low-cost method using  
12 ZnCl<sub>2</sub>/CO<sub>2</sub> activation which produced a specific capacitance of 310 F g<sup>-1</sup> in a 3-electrode  
13 system [20]. Shang *et al.*, (2021) obtained activated carbon from chitin (*Portunus*  
14 *trituberculatus* Crab) waste [21], which was converted into hierarchical porous carbon  
15 through ZIF-8 nanoparticles bio-template followed by high-temperature carbonization,  
16 leading to a specific capacitance of 182 F g<sup>-1</sup>. Similar results were also obtained from  
17 different biomass precursors such as cauliflower which produced a unique hierarchical pore  
18 structure using KOH activation at 700°C high-temperature simple which possessed a high  
19 surface area of 2061 m<sup>2</sup> g<sup>-1</sup> [22]. However, the activated carbons obtained from the above  
20 precursors are prepared in powder form, hence, they require synthetic binders and insulators  
21 to test the electrochemical properties. Although the counter electrodes used are good  
22 conduction materials, it is still considered to reduce the efficiency. Also, the template/bio-  
23 template method often used to ascertain the 3D pore structure is a relatively risky technique  
24 because the final step requires more treatment to remove the by-products. On the other hand,  
25 corn silk agricultural biomass has high potential as a hierarchical porous carbon precursor.  
26 The basic fibrous structure allows the discovery of dense nanofibers on activated carbon,  
27 thereby adding to its renewability. Although the use of corn silk as a starting material for  
28  
29  
30  
31  
32  
33  
34  
35  
36  
37  
38  
39  
40  
41  
42  
43  
44  
45  
46  
47  
48  
49  
50  
51  
52  
53  
54  
55  
56  
57  
58  
59  
60

1  
2  
3 activated carbon in supercapacitors has been previously reported, the method of preparation  
4 using binders through a relatively complicated technique is considered to limit its novelty.  
5  
6 Therefore, this study aims to prepare binder-free activated carbon through a novel one-step  
7  
8 activation of KOH/CO<sub>2</sub>. The chosen strategy has been shown to produce higher capacitance  
9  
10 compared to Mitravinda *et al.* (2018) [23] which used different methods and possesses higher  
11  
12 energy density compared to a study by Zhou *et al.* (2020) [24]. In addition, we selected  
13  
14 H<sub>2</sub>SO<sub>4</sub> aqueous electrolytes because of their advantages including the highest ionic  
15  
16 concentration, highest conductivity, and low viscosity compared to other aqueous  
17  
18 electrolytes. In result, the optimum specific capacitance of activated carbon obtained is 237 F  
19  
20 g<sup>-1</sup> with a maximum energy density of 18.19 Wh kg<sup>-1</sup> in an aqueous electrolyte of 1 M  
21  
22 H<sub>2</sub>SO<sub>4</sub>.  
23  
24  
25  
26  
27

## 28 **2. Materials and methods**

### 29 **2.1. Materials**

30  
31  
32 The corn silks (CS) were initially obtained from the traditional plantations of the  
33  
34 Kampar community, Riau and then cut into small pieces within a range of 2 cm, cleaned, and  
35  
36 sundried for 48 hours to obtain dry samples. Furthermore, the samples were pre-carbonized  
37  
38 and crushed using a crusher machine to obtain dried corn silk powder. The KOH activating  
39  
40 agent, HCl, and aqueous electrolyte H<sub>2</sub>SO<sub>4</sub> were obtained from Merck KGaA, 4271  
41  
42 Darmstadt, Germany, and Panreac Quimica Sau, Espana, while deionized water (DI) as a  
43  
44 material for neutralizing samples was made on a lab scale. The organic separator from the  
45  
46 duck eggshell membrane was extracted with 1 M HCl solution.  
47  
48  
49  
50

### 51 **2.2. Synthesis of carbon pellets**

52  
53 30 g of dried corn silks powder was dispersed with a 0.5 m/L KOH solution on a  
54  
55 hotplate at 300 rpm for 2 hours. The sample was filtered and dried in an oven at 110 °C,  
56  
57 while the corn silk powder was converted into pellets using a hydraulic press without using  
58  
59  
60

any adhesive material, hence, the adhesive properties of the pure powder were derived originally from the sample. A total of 20 pellets samples were prepared for pyrolysis using carbonization in the N<sub>2</sub> gas environment and physical activation with CO<sub>2</sub> in the furnace tube. In addition, the pyrolysis process began from a temperature of 30° C to 600 °C in N<sub>2</sub> gas and then increased to 900 °C in a CO<sub>2</sub> environment. Four different carbonization temperatures were applied namely 600 °C, 700 °C, 800 °C, and 900 °C. Moreover, to facilitate data interpretation, samples were labeled CSAC-x, CSAC was corn silk activated carbon (CSAC), while x was the number 6, 7, 8, and 9 indicating carbonization at the four temperatures. The pelleted carbon samples were neutralized using DI water.

### 2.3. Characterization of materials

The carbon pellets' density was evaluated based on changes in mass, thickness, and diameter during the pyrolysis process through standard equations. Furthermore, the amorphous properties of the samples were characterized using the XRD (X-ray diffraction) technique at an angle range of 5-60° in a Cu K $\alpha$  radiation source (Phillips expert powder instrument). Surface morphology and variation of sample elements were also examined through the SEM-EDS (Scanning electron microscopy-energy dispersive spectroscopy) technique using the JEOL-JSM-LA-3600 instrument at a voltage of 15kV. Additionally, the specific surface area and pore diversity were determined through the N<sub>2</sub> gas absorption technique and evaluated using BET and BJH calculations.

### 2.4. Supercapacitor electrochemical performance

The electrochemical properties of the supercapacitor were evaluated in two-electrode configurations. The supercapacitor cells were made in the form of sandwich layers consisting of a cell body made of acrylic, stainless steel current collector, pelleted carbon electrodes, and an organic separator from the duck eggshell membrane. Interestingly, the semi-permeable duck eggshell membrane allows the electrolyte ions to diffuse optimally on the

surface of the carbon electrode [25]. The cyclic voltammetry (CV) and galvanostatic charge-discharge (GCD) methods are techniques commonly used in evaluating specific capacitance, as well as energy and power density. CV was evaluated using the CV-UR Rad-Er 1380 instrument at a constant voltage range of 0-1.0V at a scan rate of  $1 \text{ mV s}^{-1}$ , while GCD used the 2018 CD-UR Rad-Er at a fixed current of 1 A, both instruments were calibrated with a mean error of  $\pm 6.01\%$ .

### 3. Results and discussions

Crystal phase change properties of corn silk-based hierarchical porous carbon were reviewed using the powder X-ray diffraction (XRD) method. The XRD pattern with different physical activation temperatures particularly between 700 and 900 °C, are shown in Figure 1.

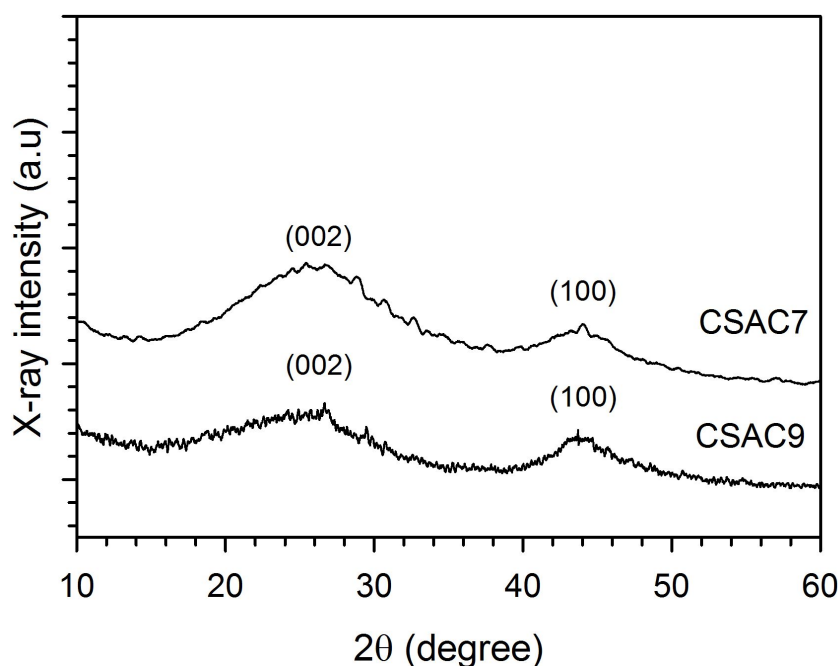


**Figure 1.** The XRD pattern of CSAC7 and CSAC9

The CSAC7 display two clearly confirmed broad peaks at  $2\theta$  angles  $24.34^\circ$  and  $43.92^\circ$  which correspond to the (002) and (100) scattering planes. These characteristics show that the structure of the turbostratic/disturbed carbon has a high amorphous nature [26]. This property is important for improving the good hierarchical pore structures in carbon samples. On the other hand, CSAC9 performed low broad peaks at angles of  $2\theta=24.86^\circ$  and  $44.13^\circ$  indicating

the amorphous nature degraded towards graphitization due to high-temperature treatment. Furthermore, the most obvious broad peaks in the (002) reflection plane ranging between angle  $24.34^{\circ}$ - $24.86^{\circ}$  indicate a random aromatic sheet structure, while the (100) reflection plane from  $43.92^{\circ}$ -  $44.13^{\circ}$  confirms the type of carbon that is close to the graphite structure, in this case, the attenuation of the graphite structure towards the formation of a disturbed carbon structure [27].

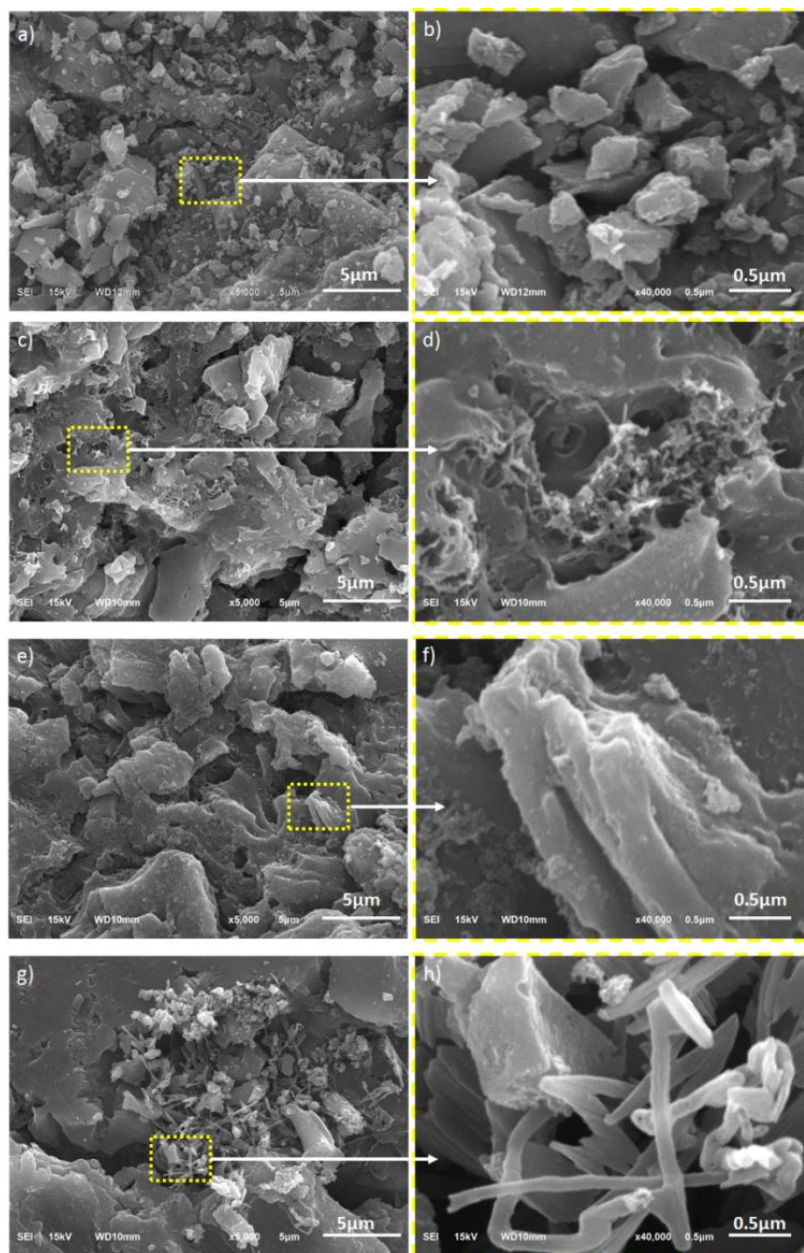


**Figure 2.** The SEM macrograph of CSAC6 in magnification of (a) 5000x, (b) 40000x, CSAC7 in magnification of (c) 5000x, (d) 40000x, CSAC8 in magnification of (e) 5000x, (f) 40000x, CSAC9 in magnification of (g) 5000x, (h) 40000x

1  
2  
3 The morphological structure of activated carbon-based corn silk waste was evaluated  
4 using the SEM method at a voltage of 15 kV. Figure 2 shows the morphological structure  
5 with different physical activation temperatures of 600, 700, 800, and 900 °C. In general, the  
6 surface structure of the sample is dominated by bulk materials, aggregation and clumps of  
7 large wrinkled particles, while some parts display a different inner surface structure for each  
8 temperature. At 600 °C (Figure 2a), the activated carbon consisted of particle aggregations  
9 with surface wrinkles. Additionally, a larger zoom in Figure 2b shows that the sample  
10 surface is relatively flat in each aggregation without any obvious pores. Furthermore,  
11 comparatively to 600 °C, physical activation at a higher temperature led to a better  
12 decomposition into the basic components such as hemicellulose, cellulose, and lignin. This  
13 indicates a relatively different surface morphology as shown in Figure 2c-d. Figure 2c shows  
14 the relatively dominant pore holes structure in the 64-7214 nm range. The diverse pore  
15 structure including mesopores and macropores were confirmed at a larger magnification area  
16 as shown in Figure 2d. Mesopores have a size ranging from 18-48 nm, while macropores are  
17 in the range of 73-136 nm. However, micropores structures were not found at this  
18 magnification. An increase in the physical activation temperature of 800 °C in the CSAC8  
19 sample shows a surface morphology filled with macropores which have a relatively large size  
20 less than 300 nm as shown in Figure 2e. In addition, Figure 2f shows a distinct morphology  
21 in which clustered tubular-rod-like structures are found. This is because the higher  
22 temperature porosity allows the breakdown of the main carbon structure derived from  
23 cellulose and lignin drastically. The rod shape is contributed from the basic structure of  
24 cellulose while the outer tubular shape is attributed to lignin [28]. This analysis has been  
25 reported in previous studies with different biomass precursors such as cassava petiole [29]  
26 and cacao shells [30]. Moreover, the temperature of 900°C maximized the basic  
27 decomposition process of cellulose and lignin to form a clear surface morphology of carbon  
28  
29  
30  
31  
32  
33  
34  
35  
36  
37  
38  
39  
40  
41  
42  
43  
44  
45  
46  
47  
48  
49  
50  
51  
52  
53  
54  
55  
56  
57  
58  
59  
60

fibers, as shown in Figure 2g-h. The diameter of the obtained nanofibers varied relatively in the range of 76 nm to 127 nm. The predominant nanofiber fiber allows well-connected pores in a relatively small size range [31]. The elemental composition of porous activated carbon samples at activation temperatures of 700 °C and 900 °C for CSAC7 and CSAC9 was examined using energy dispersive spectroscopy (EDS) techniques in the energy range of 0-20 keV. Table 1 shows the elemental composition of the CSAC7 and CSAC9 samples in detail. Elemental carbon (C) has the highest percentage of approximately 83.7485-85.2755% followed by oxygen 8.0333-8.6075%, silicon (Si) 3.2471-3.1535%, potassium (K) 1.6359-3.9428%, magnesium (Mg) 0.8317-0.7930%, and aluminum (Al) 0.4022-0.3290%.

**Table 1. The elemental composition of CSAC7 and CSAC9**

Element	CSCA7 (%)	CSAC9 (%)
Carbon (C)	85.2755	83.7485
Oxygen (O)	8.6075	8.0333
Silicon (Si)	3.2471	3.1535
Potassium (K)	1.6359	3.9428
Magnesium (Mg)	0.8317	0.7930
Aluminum (Al)	0.4022	0.3290

High-temperature pyrolysis of 700 °C for CSAC7 showed the highest carbon composition of 85.2755%. This property is considered to increase the capacitive properties of the electrode material. Furthermore, the highest elemental oxygen was also found in the CSAC7 sample which contributed to the wettability of the material thereby initiating the pseudocapacitance effect [32]. An increase in the activation temperature up to 900 °C for CSAC9 reduced the percentage of carbon and oxygen in the sample. This is because the activation of high temperatures evaporates the constituent elements of the material in the form of more H<sub>2</sub>O and CO<sub>2</sub>. Moreover, other elements such as Silicon, Potassium, Magnesium, and Aluminum are obtained in relatively low amounts from basic sources of biomass that have not been completely evaporated [33].



The analysis of N<sub>2</sub> adsorption/desorption isotherms of corn silk-based hierarchical porous activated carbon at different pyrolysis temperatures are needed to evaluate the impact of pore structure and porosity properties. Figure 3 shows the N<sub>2</sub> adsorption-desorption isotherm curve of both samples, CSAC7 had significant N<sub>2</sub> adsorption at a relative pressure of  $0.0 < P/P_0 < 0.2$ , thereby confirming the relatively large number of micropores.

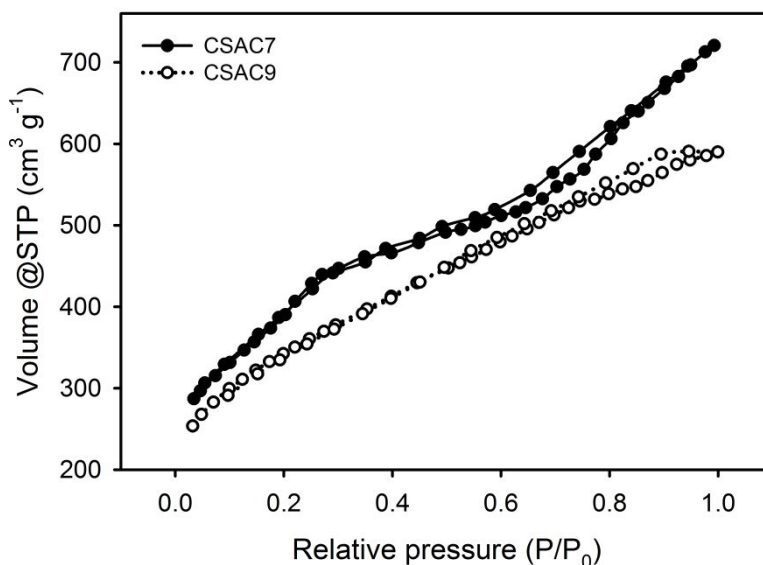


**Figure 3.** Nitrogen adsorption-desorption isotherms of CSAC7 and CSAC9

**Table 2.** Specific surface area, pore volume and average pores size of CSAC7 and CSAC9

Sample	$S_{\text{BET}}$ ( $\text{m}^2 \text{g}^{-1}$ )	$S_{\text{micro}}$ ( $\text{m}^2 \text{g}^{-1}$ )	$S_{\text{meso}}$ ( $\text{m}^2 \text{g}^{-1}$ )	$V_{\text{tot}}$ ( $\text{cm}^3 \text{g}^{-1}$ )	$V_{\text{micro}}$ ( $\text{cm}^3 \text{g}^{-1}$ )	$V_{\text{meso}}$ ( $\text{cm}^3 \text{g}^{-1}$ )	$D_{\text{aver}}$ (nm)
CSAC7	1096.951	531.087	565.864	1.115	0.314	0.801	4.06
CSAC9	744.818	423.360	321.458	0.9126	0.4476	0.465	3.15

Furthermore, the H4 type hysteresis loop was clearly shown over a relatively long relative pressure range of  $0.2 < P/P_0 < 0.9$  indicating uniform mesoporous characteristics at CSAC7 as presented in Table 2. The tail at high-pressure  $P/P_0 > 0.9$  shows the presence of macropores, but the addition of the physical activation temperature up to 900°C in CSAC9 showed a different N<sub>2</sub> isotherm absorption compared to CSAC7. The N<sub>2</sub> adsorption-desorption curve of CSAC9 shows a relatively linearly increasing adsorption which is not too high at low pressure, thereby indicating the presence of low micropores. In addition, the H4 type hysteresis loop is not formed completely at a relatively short pressure range of  $P/P_0 = 0.6$  to 0.95 which is mainly due to the pores growing towards the larger one and is dominated by narrow bottle neck-like types with a larger inner surface [34] as shown in Table 2. The pore

size distribution as presented in Figure 4 show that both samples have a combination of micropores and macropores. This result is relatively consistent with SEM which also confirms the hierarchical porous structure. CSAC7 has a structure of hierarchically connected 3D pores leading to the presence of mesopores with a peak at 3.89 nm. Furthermore, the chemical impregnation of KOH at 700 °C high-temperature pyrolysis allows the precursor to produce a good combination of micropores and mesopores to improve the performance of the base electrode.

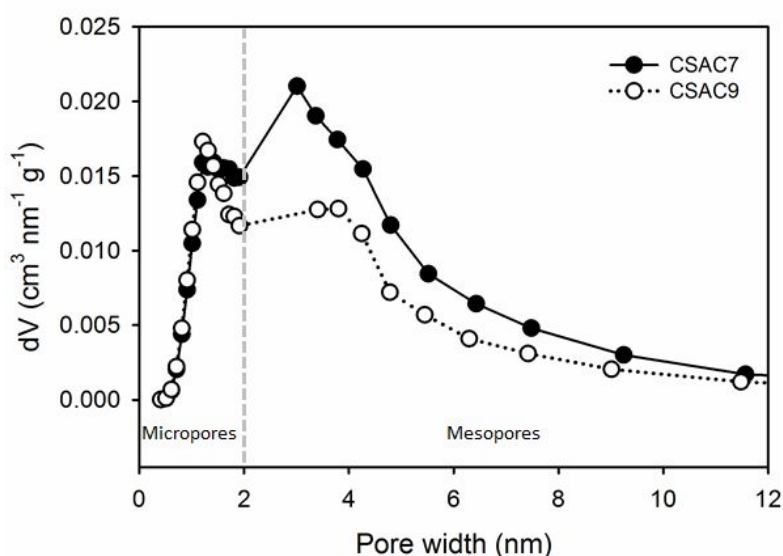


**Figure 4.** Pore sizes profile of CSAC7 and CSAC9

The microporous and mesoporous percentages of CSAC7 were 48.41% and 51.59% with a high surface area of 1096.951 m<sup>2</sup> g<sup>-1</sup>. The high surface area coupled with the combination of the hierarchically connected pores is believed to improve the electrochemical properties of supercapacitors [35]. In addition, the high mesoporous volume fraction potentially facilitates rapid ion transport and act as an electrolyte ion reservoir, thereby reducing the ion diffusion distance to the carbon surface, ensuring high rate capability and high power density. Moreover, CSAC9 displays a relatively similar pore size distribution with CSAC7 but is dominated by micropores with a percentage of 56.84%. KOH impregnation at higher temperatures up to 900°C allows degradation of carbon aggregation and erodes the main pore walls, thereby creating tubular and nanofiber structures. This simultaneously reduces the

specific surface area of CSAC9 to  $744.818 \text{ m}^2 \text{ g}^{-1}$  with an average diameter of  $3.15 \text{ nm}$  as shown in Table 2. Nevertheless, the developed porosity properties of carbon materials are important for electrolyte ions' rapid transport and penetration [36]. These results are consistent with the SEM and density data.

The main parameters used to evaluate the electrochemical properties of hierarchical porous activated carbon include high specific capacitance, increased energy and fixed power density, as well as retention capacitance. Based on the  $\text{N}_2$  gas absorption analysis, the corn silk-based activated carbon has a combination of micropores and mesopores that is able to accommodate a relatively high charge of active ions and facilitate diffusion without obstruction at the electrode/electrolyte interface. The electrochemical performance of CSAC6, CSAC7, CSAC8, and CSAC9 based on different physical activation temperatures was evaluated with a two-electrode configuration in an aqueous electrolyte using cyclic voltammetry and galvanostatic charge-discharge techniques. Cyclic voltammetry (CV) curves at 600, 700, 800, and 900 °C are shown in Figure 5. The CV profile exhibits a quasi-rectangular shape, indicating the typical behavior of electrochemical double-layer type supercapacitors (EDLC) in an aqueous electrolytic system at a scan rate of  $1 \text{ mV s}^{-1}$ .

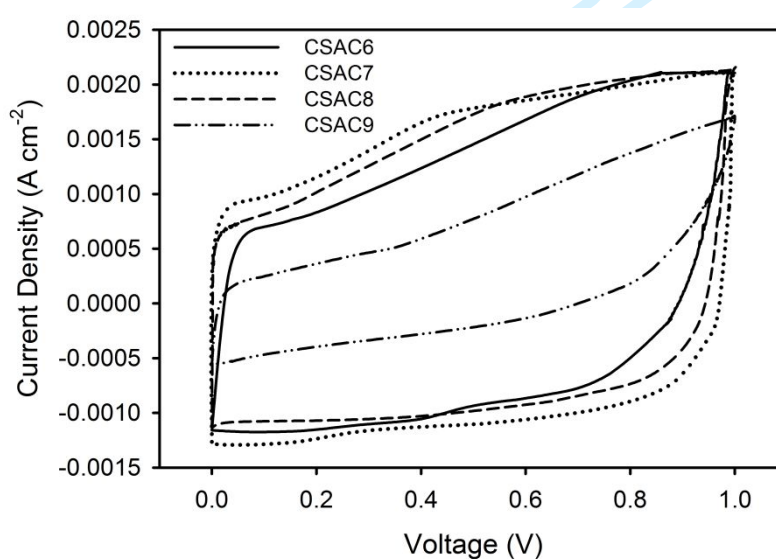


**Figure 5.** CV curve of CSAC6, CSAC7, CSAC8, and CSAC9

In addition, the pseudocapacitance property was found to be relatively low as indicated by a spike in current density of the voltage ranging from 0.3-0.6V. This property is a contribution of the heteroatom and wettability properties of elemental oxygen in the sample. In general, all samples exhibited similar electrochemical properties. By using standard equations, the specific capacitances of CSAC6, CSAC7, CSAC8, and CSAC9 was evaluated to be 184, 211, 194, and 143 F g<sup>-1</sup>, respectively. An increase in the physical activation temperature improved the capacitive properties of the supercapacitor by 211 F g<sup>-1</sup>. This is because the higher temperature of CSAC7 showed a relatively rich surface structure of mesopores and macropores, which provides a high surface area and diffusion path of ionic charge in all directions, thereby facilitating the high capacitive properties. This analysis is consistent with SEM results and N<sub>2</sub> gas absorption in Figures 2 and 3. At 800 °C, the surface structure of the capacitive properties was reduced to 194 F g<sup>-1</sup>. This is because the increase in the physical activation temperature in the CSAC8 sample shows a surface morphology filled with macropores with a relatively large size less than 300 nm, as shown in Figure 2e. In addition, the morphology of the clustered tubular rod-like structure allows for fractures that narrow the ion transport pathways on the electrode surface.

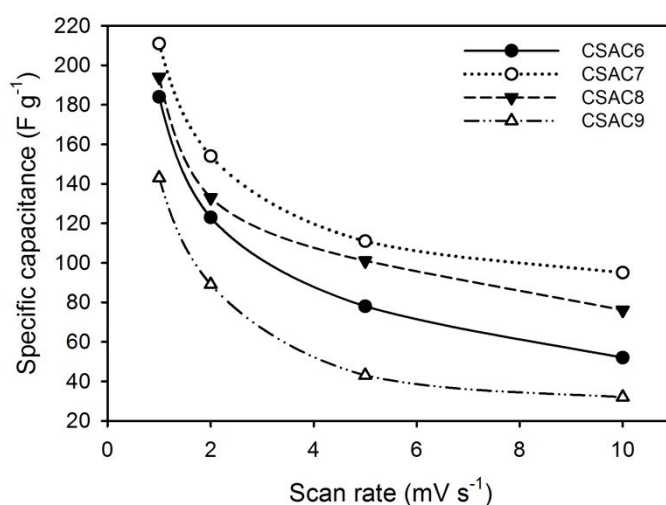


**Figure 6.** The curve of specific capacitance vs. scan rate of CSAC6, CSAC7, CSAC8, and CSAC9

1  
2  
3 A further temperature is increased up to 900 °C for CSAC9 allows the erosion and  
4 breakdown of the particle walls of carbon aggregation and rod-like structures to cover the  
5 existing pores, this reduced the capacitive properties to 143 F g<sup>-1</sup>. Although the pore structure  
6 displays relatively dense nanofibers, as shown in Figure 2h, it is unable to maintain the 3D  
7 hierarchical pore distribution of micropores and mesopores thereby reducing the  
8 electrochemical properties. The specific capacitances of CSAC6, CSAC7, CSAC8, and  
9 CSAC9 were also evaluated at different scan rates from 1 mV s<sup>-1</sup> to 10 mV s<sup>-1</sup>, as shown in  
10 Figure 6. The activated carbon which maintained the highest specific capacitance of 45% was  
11 CSAC7, followed by CSAC8, CSAC6, and CSAC9 with values of 39%, 28%, and 23%,  
12 respectively. The galvanostatic charge-discharge (GCD) curves of symmetric cells CSAC6,  
13 CSAC7, CSAC8, and CSAC9 at a current density of 1 A g<sup>-1</sup> are shown in Figure 7a. In  
14 general, the GCD curve displays a normal profile for the EDLC type with a slightly faint iR  
15 drop. According to the GCD profile, the specific capacitances produced at CSAC6, CSAC7,  
16 CSAC8, and CSAC9 were 152, 237, 174 and 124 F g<sup>-1</sup>, respectively, in the electrolyte of 1 M  
17 H<sub>2</sub>SO<sub>4</sub>. Higher activation temperature from 600°C to 700°C confirmed micro-mesopores  
18 combinations of 48.41% and 51.59% displayed the highest electrochemical properties from  
19 152 F g<sup>-1</sup> to 237 F g<sup>-1</sup>. These results correlate with SEM, N<sub>2</sub> gas adsorption/desorption, and  
20 CV analysis. The high activation temperature of from 700°C to 900°C decreased the  
21 capacitive value of the carbon electrode up to 124 F g<sup>-1</sup> for the CSAC9 sample. This is  
22 associated with the collapse of the pore walls and the erosion of the carbon framework  
23 structure to cover the active site of the ionic charge below [34].  
24  
25  
26  
27  
28  
29  
30  
31  
32  
33  
34  
35  
36  
37  
38  
39  
40  
41  
42  
43  
44  
45  
46  
47  
48  
49  
50  
51  
52  
53  
54  
55  
56  
57  
58  
59  
60

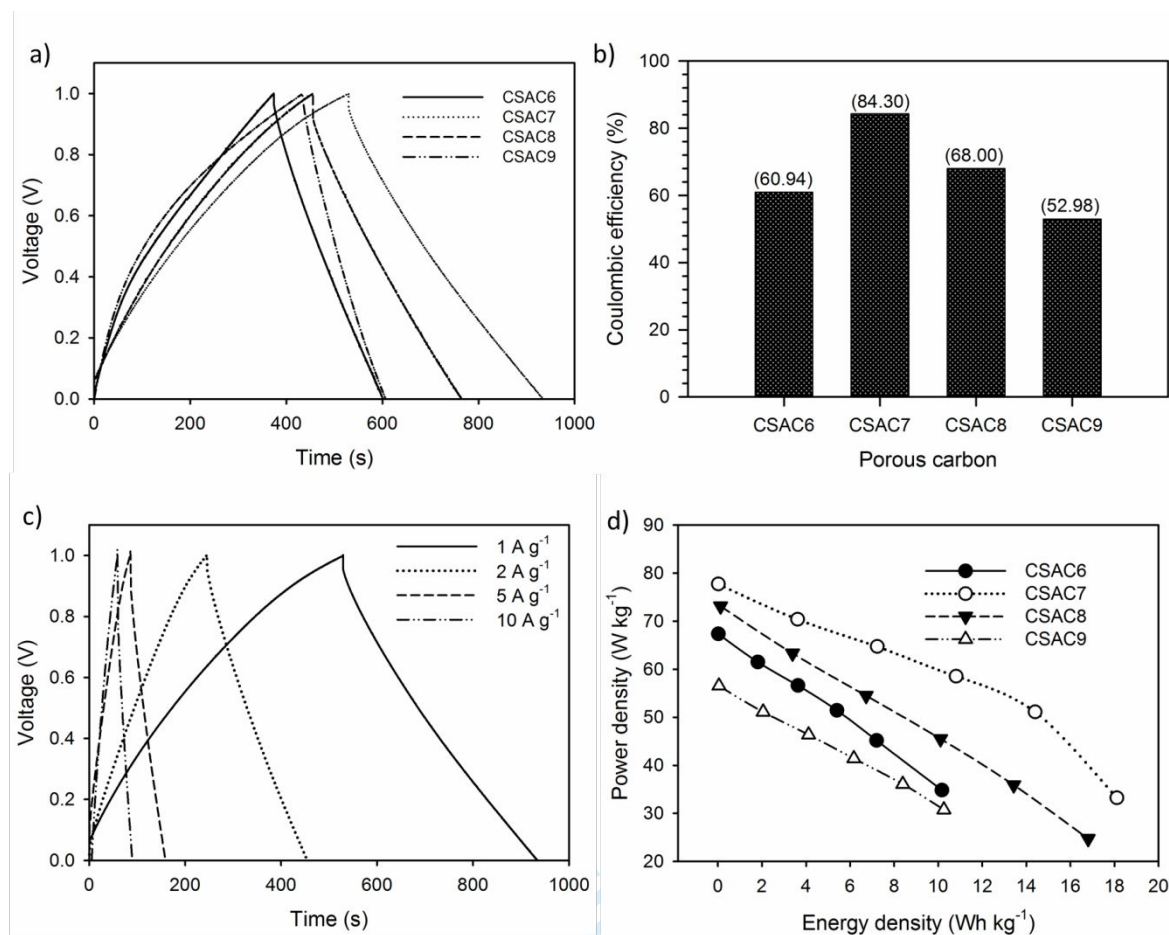


**Figure 7.** (a) GCD curve, (b) Coulombic efficiency of CSAC6, CSAC7, CSAC8, and CSAC9 (c) GCD curve at different current density of CSAC7, and (d) Ragone plot of CSAC6, CSAC7, CSAC8, and CSAC9 in 1 M H<sub>2</sub>SO<sub>4</sub> electrolyte

Furthermore, the resistance in CSAC7 was lower at 0.0025Ω due to the relatively high dominance of the mesopores which improved the diffusion of ionic charges in all directions compared to CSAC6, CSAC8, and CSAC9 which has a higher resistance value of 0.012, 0.27, and 0.034 Ω, respectively. This is also contributed by the semi-permeable duck eggshell membrane which allows the electrolyte ions to diffuse optimally on the surface of the carbon electrode [25]. In addition, the charge and discharge times on the GCD profiles reflect the coulombic efficiency of GLACs, as shown in Figure 7b. CSAC7 had the highest coulombic efficiency of about 84.30%, followed by CSAC8, CSAC6 and CSAC9 68.00%, 60.94 and 52.98%, respectively which confirmed confirming the high collective interpenetration and

accessibility of the electrolytes. Moreover, the GCD profile of CSAC7 was reviewed at different current density of 1, 2, 5, and 10 A g<sup>-1</sup>, as shown in Figure 7c. It can be noted that the GCD curves of CSAC7 still maintain primary symmetric triangle shape at 10 A g<sup>-1</sup> suggesting stable double-layer capacitor behaviors, fast ion response, and low internal resistance in EDL processes <sup>42</sup>. At 1 A g<sup>-1</sup>, CSAC7 sample delivers a specific capacitance of 237 F g<sup>-1</sup> and it still maintains 210 F g<sup>-1</sup> at 10 A g<sup>-1</sup>, initiating a high-rate performance of 88.6%.

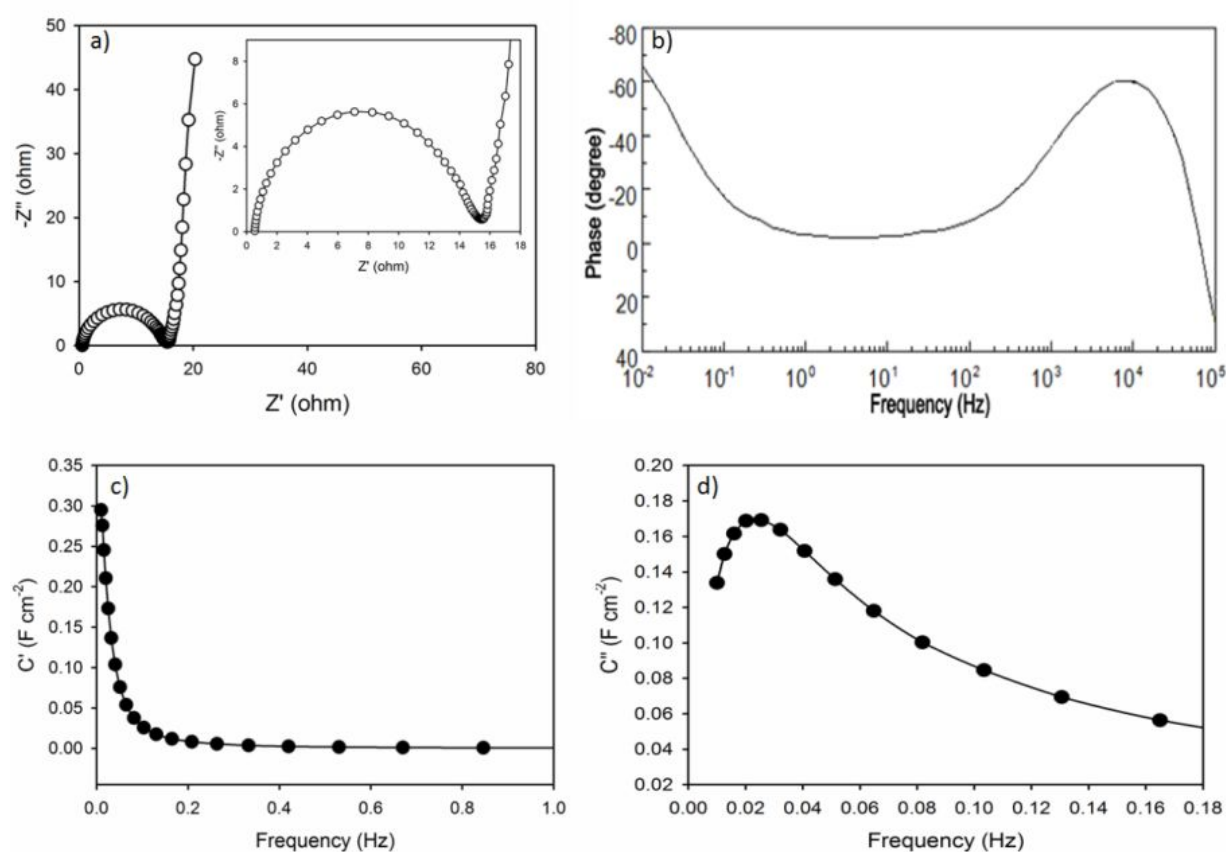


**Figure 8.** (a) Nyquist plot, (b) Bode phase angle plot, (c) real capacitance ( $C'$ ) vs. frequency plot, and (d) imaginer capacitance ( $C''$ ) vs. frequency plot of CSAC7 symmetrical devices

To compare the performance of both samples in-depth, Ragone plots were used to evaluate the energy and power density which are calculated using standard formulas as shown in Figure 7c. Symmetrical supercapacitors CSAC6, CSAC7, CSAC8 and CSAC9 assembled

1  
2  
3 with an aqueous electrolyte of 1M H<sub>2</sub>SO<sub>4</sub> in an organic separator had energy densities of  
4  
5 10.1712, 18.1081, 16.8049 and 10.2596 Wh kg<sup>-1</sup> as well as power densities of 67.3793,  
6  
7 77.74, 73.1373 and 56.5421 W kg<sup>-1</sup>, respectively. The high electrochemical capability of  
8  
9 CSAC7 is due to the 3D hierarchical porous structure and the specific surface area which  
10  
11 provides a short and accessible ion transfer area in all directions for ionic charges to diffuse at  
12  
13 the electrode/electrolyte interface.  
14  
15

16  
17 The high electrochemical confirmation of CSAC7 was reviewed in depth via a Nyquist  
18  
19 Plot with a limited diffusion area in the frequency range of 0.01 Hz to 100,000 Hz, as shown  
20  
21 in Figure 8a. Horizontal translation along the Z' axis confirms a relatively low R<sub>s</sub> 0.87 Ωcm<sup>2</sup>  
22  
23 indicating a good ions adsorption and desorption process at the electrode-electrolyte  
24  
25 interface. Furthermore, the RCT (12.3 Ωcm<sup>2</sup>) interpreted at the semicircular position  
26  
27 confirmed the fast charge transfer kinetically as a result of the current passing through the  
28  
29 electrode forming an electric layer. This is due to the hierarchical pores structure with a  
30  
31 combination of micro, meso, and macropores initiates the active site which is followed by the  
32  
33 ability of ion diffusion in all directions without any obstacles. In addition, the straight line  
34  
35 that tends to be perpendicular at low frequencies confirms the pure capacitive and high ion  
36  
37 transfer rate at the CSAC7 electrode. The Bode phase angle plot of CSAC7 was also  
38  
39 evaluated as shown in Figure 8b. The phase angle at low frequencies reveals specific  
40  
41 information about the ability of the electrode to generate an electric double layer. CSAC7  
42  
43 electrode displays a phase angle close to -90° indicating that the normal dielectric layer of the  
44  
45 EDLC version is accompanied by impaired ion degradation due to self-heteroatom doping. In  
46  
47 addition, the Bode phase angle plot provides further information for the characteristics of the  
48  
49 conductive material through analysis of the real capacitance (C') and the imaginary  
50  
51 capacitance (C'') with respect to frequency, as shown in Figures 8b, and 8c. The C' values are  
52  
53 weak in the lower frequency and higher frequency regions, the C' values show less frequency  
54  
55  
56  
57  
58  
59  
60



1  
2  
3 dependence, indicating a purely resistive behavior in CSAC7. Moreover, the value of the  
4  
5 imaginary capacitance  $C''$  at the peak frequency confirms a relaxation time of 9.25 seconds,  
6  
7 indicating that the symmetrical CSAC7 device acts as a pure capacitor. This value indicates a  
8  
9 measure of how quickly the stored energy of the device can be efficiently distributed. For  
10  
11 comparison, the obtained carbon nanofiber-based on corn silk waste showed higher  
12  
13 electrochemical properties than the carbon nanofiber-based on bacterial cellulose and tofu  
14  
15 dregs obtained through chemical activation of KOH and  $H_3PO_4$  [37,38]. In addition, although  
16  
17 polymer-based carbon nanofibers exhibit superior specific capacitance, our study was able to  
18  
19 produce higher energy densities than the previously reported as confirmed in referee [39].  
20  
21 This is due to the combination of nanofiber and micro-mesoporous structures allowing the  
22  
23 provision of high active sites and ion-transport channels. Moreover, the binder-free electrode  
24  
25 design supports the high electrochemical performance of the supercapacitor.  
26  
27  
28  
29

#### 30 **4. Conclusion**

31  
32  
33 Based on the results, hierarchically porous carbon nanofiber was successfully obtained  
34  
35 from corn silk using a low-cost, simple, and sustainable technique without a binding material  
36  
37 for a high energy density of symmetric supercapacitors. In addition, different physical  
38  
39 activation temperatures display distinctive pores structure with individual advantages. At 700  
40  
41 °C, a 3D hierarchical pore structure was displayed followed by a high surface area leading to  
42  
43 the formation of an ideal combination of micro and mesopores for enhancing the high  
44  
45 performance of the electrode material. Using a two-electrode binder-free system, CSAC7  
46  
47 showed the best electrochemical properties with a specific capacitance of  $237 \text{ F g}^{-1}$  in a 1 M  
48  
49  $H_2SO_4$  aqueous electrolyte. Hence, the maximum energy density of  $18.19 \text{ Wh kg}^{-1}$  and  
50  
51 power density of  $77.74 \text{ W kg}^{-1}$  at current density of  $1 \text{ A g}^{-1}$ . This result shows that the  
52  
53 approach applied in this study confirmed the potential of corn silk as an activated carbon  
54  
55 based material with high properties.  
56  
57  
58  
59  
60

## Acknowledgement

This study was funded by the collaborative grants between universities, State Islamic University of Sultan Syarif Kasim Riau with contract No. 873/Un.04/L. 1/TL.01/03/2022.

## References

- [1] Poonam, Sharma K, Arora A and Tripathi S K 2019 Review of supercapacitors: Materials and devices *J. Energy Storage* **21** 801–25
- [2] Kumar R, Sahoo S, Joanni E, Singh R K, Tan W K, Kar K K and Matsuda A 2019 Recent progress in the synthesis of graphene and derived materials for next generation electrodes of high performance lithium ion batteries *Prog. Energy Combust. Sci.* **75** 100786
- [3] Farma R, Anugrah A P, Apriyani I and Awitdrus A 2022 Facile synthesis of Veitchia merilli coir-based porous carbon using combined chemical and physical activation routes as electrode material for energy storage *Adv. Nat. Sci.: Nanosci. Nanotechnol.* **13** 015009
- [4] Hoa L T M 2021 Surface functionalisation of multi-walled carbon nanotubes with tris(2-aminoethyl)amine and their characterisation *Adv. Nat. Sci.: Nanosci. Nanotechnol.* **12** 025014
- [5] Chaudhary S, Raja M and Sinha O P 2021 A review on the different types of electrode materials for aqueous supercapacitor applications *Adv. Nat. Sci.: Nanosci. Nanotechnol.* **12** 015011
- [6] Zheng S, Li Q, Xue H, Pang H and Xu Q 2020 A highly alkaline-stable metal oxide@metal–organic framework composite for high-performance electrochemical energy storage *National Science Review* **7** 305–314
- [7] Tiwari S K, Sahoo S, Wang N and Huczko A 2020 Graphene research and their outputs: Status and prospect *J. Sci. Adv. Mater. Devices* **5** 10–29
- [8] Taer E and Taslim R 2018 Brief Review: Preparation Techniques of Biomass Based Activated Carbon Monolith Electrode for Supercapacitor Applications *AIP Conference Proceedings* **1927** 020004-1-020004–4
- [9] Bhat V S, Kanagavalli P, Sriram G, B R P, John N S, Veerapandian M, Kurkuri M and Hegde G 2020 Low cost, catalyst free, high performance supercapacitors based on porous nano carbon derived from agriculture waste *J. Energy Storage* **32** 101829
- [10] Gallay P, López-Mujica M, Ortiz E, Zhang Y, Perrachione F, Montemerlo A, Galicia L, Bedioui F, Rodriguez M, Dalmaso P, Rubianes M, Gutierrez F, Eguílaz M and Rivas G 2020 Carbon Nanomaterials-Based Electrochemical Biosensors for the Quantification of High Impact Biomarkers *Meet. Abstr.* **MA2020-01** 1893
- [11] Wang D, Nai J, Li H, Xu L and Wang Y 2019 A robust strategy for the general synthesis of hierarchical carbons constructed by nanosheets and their application in high performance supercapacitor in ionic liquid electrolyte *Carbon* **141** 40–49
- [12] Wang D, Pan Z, Chen G, and Lu Z 2021 Glycerol derived mesopore-enriched hierarchically carbon nanosheets as the cathode for ultrafast zinc ion hybrid supercapacitor applications *Electrochim. Acta* **379** 13817
- [13] Mehare M D, Deshmukh A D and Dhoble S J 2020 Preparation of porous agro-waste-derived carbon from onion peel for supercapacitor application *J. Mater. Sci.* **55** 4213–24
- [14] Sodtipinta J, Ieosakulrat C, Poonyayant N, Kidkhunthod P, Chanlek N, Amornsakchai T and Pakawatpanurut P 2017 Interconnected open-channel carbon nanosheets derived

- 1  
2  
3 from pineapple leaf fiber as a sustainable active material for supercapacitors *Ind.*  
4 *Crops Prod.* **104** 13–20
- 5 [15] Chen Z, Wang X, Xue B, Li W, Ding Z, Yang X, Qiu J and Wang Z 2020 Rice husk-  
6 based hierarchical porous carbon for high performance supercapacitors : The structure-  
7 performance relationship *Carbon N. Y.* **161** 432–44
- 8 [16] Liangshuo L, Lin Q, Xinyu L, Ming D and Xin F 2020 Preparation of biomass-based  
9 porous carbon derived from waste ginger slices and its electrochemical performance  
10 *Optoelectron. Adv. Mater. Rapid Commun.* **14** 548–55
- 11 [17] He X, Li R, Han J, Yu M and Wu M 2013 Facile preparation of mesoporous carbons  
12 for supercapacitors by one-step microwave-assisted ZnCl<sub>2</sub> activation *Mater. Lett.* **94**  
13 158–60
- 14 [18] Taer E, Pratiwi L, Apriwandi, Mustika W S, Taslim R and Agustino 2020 Three-  
15 dimensional pore structure of activated carbon monolithic derived from hierarchically  
16 bamboo stem for supercapacitor application *Commun. Sci. Technol.* **5** 22–30
- 17 [19] Yang V, Senthil R A, Pan J, Kumar T R, Sun Y and Liu X 2020 Hierarchical porous  
18 carbon derived from jujube fruits as sustainable and ultrahigh capacitance material for  
19 advanced supercapacitors *J. Colloid Interface Sci.* **579** 347–56
- 20 [20] Jiang X, Guo F, Jia X, Zhan Y, Zhou H and Qian L 2020 Synthesis of nitrogen-doped  
21 hierarchical porous carbons from peanut shell as a promising electrode material for  
22 high-performance supercapacitors *J. Energy Storage* **30** 101451
- 23 [21] Shang Z, An X, Liu L, Yang J, Zhang W, Dai H, Cao H, Xu Q, Liu H and Ni Y 2021  
24 Chitin nanofibers as versatile bio-templates of zeolitic imidazolate frameworks for N-  
25 doped hierarchically porous carbon electrodes for supercapacitor *Carbohydr. Polym.*  
26 **251** 117107
- 27 [22] Men B, Guo P, Sun Y, Tang Y, Chen Y, Pan J and Wan P 2019 High-performance  
28 nitrogen-doped hierarchical porous carbon derived from cauliflower for advanced  
29 supercapacitors *J. Mater. Sci.* **54** 2446–57
- 30 [23] Mitravinda T, Nanaji K, Anandan S, Jyothirmayi A, Chakravadhanula V S K, Sharma  
31 C S and Rao T N 2018 Facile Synthesis of Corn Silk Derived Nanoporous Carbon for  
32 an Improved Supercapacitor Performance *J. Electrochem. Soc.* **165** A3369–79
- 33 [24] Zhou J, Yuan S, Lu C, Yang M and Song Y 2020 Hierarchical porous carbon  
34 microtubes derived from corn silks for supercapacitors electrode materials *J.*  
35 *Electroanal. Chem.* **878** 114704
- 36 [25] Li W, Chen C, Wang H, Li P, Jiang X, Yang J and Liu J 2022 Hierarchical porous  
37 carbon induced by inherent structure of eggplant as sustainable electrode material for  
38 high performance supercapacitor *J. Mater. Res. Technol.* **17** 1540–52
- 39 [26] Ni W and Shi L 2019 Review Article: Layer-structured carbonaceous materials for  
40 advanced Li-ion and Na-ion batteries: Beyond graphene *J. Vacuum Science &*  
41 *Technology A* **37** 040803
- 42 [27] Serafin J, Baca M, Biegun M, Mijowska E, Kaleńczuk R J, Sreńscek-Nazzal J and  
43 Michalkiewicz B 2019 Direct conversion of biomass to nanoporous activated  
44 biocarbons for high CO<sub>2</sub> adsorption and supercapacitor applications *Appl. Surf. Sci.*  
45 **497** 143722
- 46 [28] Jiang W, Pan J and Liu X 2019 A novel rod-like porous carbon with ordered  
47 hierarchical pore structure prepared from Al-based metal-organic framework without  
48 template as greatly enhanced performance for supercapacitor *J. Power Sources* **409**  
49 13–23
- 50 [29] Taer E, Apriwandi, Dalimunthe B K L and Taslim R 2021 A rod-like mesoporous  
51 carbon derived from agro-industrial cassava petiole waste for supercapacitor  
52 application *J. Chem. Technol. Biotechnol.* **96** 662–71
- 53  
54  
55  
56  
57  
58  
59  
60

- 1  
2  
3 [30] Taer E, Apriwandi A, Agutino A, Taslim R, Mustika W S and Exa Fadli 2021 Surface  
4 modification: unique ellipsoidal/strobili-fiber structure of porous carbon monolith for  
5 electrode supercapacitor *Nanosci. Technol. An Int. J.* **12** 45–63
- 6 [31] Ni W, Shi L and Resol 2022 Vegetable Fibers Composites *Materials Research*  
7 *Foundations* **122** 154-198
- 8 [32] Liu F, Wang Z, Zhang H, Jin L, Chu X, Gu B, Huang H and Yang W 2019 Nitrogen,  
9 oxygen and sulfur co-doped hierarchical porous carbons toward high-performance  
10 supercapacitors by direct pyrolysis of kraft lignin *Carbon N. Y.* **149** 105–16
- 11 [33] Zhou D-D, Zhang X-W, Mo Z-W, Xu Y-Z, Tian X-Y, Li Y, Chen X-M and Zhang J-  
12 P 2019 Adsorptive separation of carbon dioxide: From conventional porous materials  
13 to metal–organic frameworks *EnergyChem* **1** 100016
- 14 [34] Bai Y, Liu C, Chen T, Li W, Zheng S, Pi Y, Luo Y and Pang H 2021 MXene-  
15 Copper/Cobalt Hybrids via Lewis Acidic Molten Salts Etching for High Performance  
16 Symmetric Supercapacitors *Angew. Chem. Int. Ed.* **60** 25318
- 17 [35] Surya K and Michael M S 2020 Novel interconnected hierarchical porous carbon  
18 electrodes derived from bio-waste of corn husk for supercapacitor applications *J.*  
19 *Electroanal. Chem.* **878** 114674
- 20 [36] Wang Y, Qiao M and Mamat X 2021 Nitrogen-doped macro-meso-micro hierarchical  
21 ordered porous carbon derived from ZIF-8 for boosting supercapacitor performance  
22 *Appl. Surf. Sci.* **540** 148352
- 23 [37] Hao X, Wang J, Ding B, Wang Y, Chang Z, Dou H and Zhang X 2017 Bacterial-  
24 cellulose-derived interconnected meso-microporous carbon nanofiber networks as  
25 binder-free electrodes for high-performance supercapacitors *J. Power Sources* **352** 34–  
26 41
- 27 [38] Taer E, Hasanah F and Taslim R 2021 Nanofiber-enrich activated carbon coin derived  
28 from tofu dregs as electrode materials for supercapacitor *Commun. Sci. Technol.* **6** 41–  
29 8
- 30 [39] Li J, Zou Y, Xiang C, Xu F, Sun L, Li B and Zhang J 2021 Osmanthus fragrans-  
31 derived N-doped porous carbon for supercapacitor applications *J. Energy Storage* **42**  
32 103017
- 33  
34  
35  
36  
37  
38  
39  
40  
41  
42  
43  
44  
45  
46  
47  
48  
49  
50  
51  
52  
53  
54  
55  
56  
57  
58  
59  
60



Rika Taslim &lt;rikataslim@gmail.com&gt;

---

**[ANSN-2022-0119.R1] - Decision on Manuscript: ACCEPTED**

1 message

---

**NQL Editor-in-Chief** <onbehalf@manuscriptcentral.com>

Sun, Sep 11, 2022 at 3:56 PM

Reply-To: [ansn.eic@vast.vn](mailto:ansn.eic@vast.vn)To: [rikataslim@gmail.com](mailto:rikataslim@gmail.com)

11-Sep-2022

Dear Dr. Taslim:

It is a pleasure to accept your manuscript entitled "Agricultural Bio-waste of Corn Silk derived Porous Carbon for High-performance Supercapacitors" in its current form for publication in the Advances in Natural Sciences: Nanoscience and Nanotechnology (ANSN).

Your manuscript is now transferring to the production process. For the production editing, all source figures/sub-figures must be in high resolution graphic format (TIFF/PNG/JPEG), ex. figure\_1a.tif, figure\_1b.jpg, Figure\_2.png... These figures should be split into the individual files and then archived in a single zip file. Please send us the compressed file including the source manuscript (Word or LaTeX) at [journal@ans.vast.vn](mailto:journal@ans.vast.vn).

When your page proofs are ready for your review, you will receive an email from IOP Publishing with instructions for downloading your page proofs. You will have only two business days to review the proofs and respond with any required corrections before the paper is finalized for publication.

Thank you for giving us the opportunity to learn about your work. On behalf of the Editors of the Advances in Natural Sciences: Nanoscience and Nanotechnology, we look forward to your continued contributions to the Journal. If you have any questions, feel free to contact us at [journal@ans.vast.vn](mailto:journal@ans.vast.vn).

Sincerely,

Editor-in-Chief

Advances in Natural Sciences: Nanoscience and Nanotechnology (ANSN)

Jointly published by VAST (VN) and IOP (UK)

Abstracted in Web of Science (ESCI), Scopus, Chemical Abstracts,...

E-mail: [journal@ans.vast.vn](mailto:journal@ans.vast.vn)Homepage: <https://iopscience.iop.org/ansn>; <https://ans.vast.vn/>Manuscript submission: <https://mc04.manuscriptcentral.com/vastansn>

---

**[ANSN-2022-0119.R1] - Please Submit Copyright Agreement**

1 message

---

**NVT Secretariat of ANSN** <onbehalfof@manuscriptcentral.com>

Sun, Sep 11, 2022 at 3:56 PM

Reply-To: journal@ans.vast.vn

To: rikataslim@gmail.com

11-Sep-2022

Dear Dr. Rika Taslim,

Please submit the copyright agreement for your recently accepted manuscript, ANSN-2022-0119.R1, to Advances in Natural Sciences: Nanoscience and Nanotechnology (ANSN) as soon as possible. You can use the link below to go directly to your Advances in Natural Sciences: Nanoscience and Nanotechnology Author Center to fill the form.

[https://mc04.manuscriptcentral.com/vastansn?URL\\_MASK=ac8883527ef54b00a8a142cdefd0f9e6](https://mc04.manuscriptcentral.com/vastansn?URL_MASK=ac8883527ef54b00a8a142cdefd0f9e6)

If you have any questions, feel free to contact us at [journal@ans.vast.vn](mailto:journal@ans.vast.vn).

Sincerely,

Editorial Office

Advances in Natural Sciences: Nanoscience and Nanotechnology (ANSN)

Jointly published by VAST (VN) and IOP (UK)

Abstracted in Web of Science (ESCI), Scopus, Chemical Abstracts,...

E-mail: [journal@ans.vast.vn](mailto:journal@ans.vast.vn)Homepage: <https://iopscience.iop.org/ansn>; <https://ans.vast.vn/>Manuscript submission: <https://mc04.manuscriptcentral.com/vastansn>



Rika Taslim &lt;rikataslim@gmail.com&gt;

---

**The final version of record for your article for Advances in Natural Sciences: Nanoscience and Nanotechnology is now available**

1 message

---

**customerservices@iopublishing.org** <customerservices@iopublishing.org>

Tue, Nov 1, 2022 at 10:51 AM

To: rikataslim@gmail.com



Dear Rika Taslim

Re: "Agricultural bio-waste of corn silk-derived porous carbon for high-performance supercapacitors" by Taslim et al

We are pleased to let you know that the final version of record of your article has now been published to IOPscience and can be found online at <https://doi.org/10.1088/2043-6262/ac9c52>. Please note that it can take up to an hour for your article to be indexed via CrossRef and therefore the DOI link in this email may not resolve immediately.

You can also find the PDF version of your article [here](#)

Please note that the link for your PDF will only be valid for 7 days after receiving this email.

We appreciate your contribution to *Advances in Natural Sciences: Nanoscience and Nanotechnology*

IOP Publishing  
Temple Circus, Temple Way, Bristol, BS1 6HG, UK  
[iopscience.iop.org/journals](https://iopscience.iop.org/journals)



This email (and attachments) are confidential and intended for the addressee(s) only. If you are not the intended recipient please notify the sender, delete any copies and do not take action in reliance on it. Any views expressed are the author's and do not represent those of IOP, except where specifically stated. IOP takes reasonable precautions to protect against viruses but accepts no responsibility for loss or damage arising from virus infection. For the protection of IOP's systems and staff emails are scanned automatically.

**IOP Publishing Limited** Registered in England under Registration No 467514. Registered Office: Temple Circus, Temple Way, Bristol BS1 6HG England VAT No GB 461 6000 84. Please consider the environment before printing this e-mail.